Thermal and Non-Thermal Atmospheric Plasma in Cancer Treatment

by Eda Gjika

B.Sc. in Chemistry, May 2011, University of Southern Maine

A Dissertation submitted to

The Faculty of
The School of Engineering and Applied
Science of the George Washington University
in partial fulfillment of the requirements for
the degree of Doctor of Philosophy

August 31, 2019

Dissertation directed by

Michael Keidar
Professor of Mechanical & Aerospace Engineering

Mary Ann Stepp
Professor of Anatomy and Regenerative Biology and of Ophthalmology

The School of Engineering and Applied Science of The George Washington University certifies that Eda Gjika has passed the Final Examination for the degree of Doctor of Philosophy as of July 22, 2019 of dissertation defense. This is the final and approved form of the dissertation.

Thermal and Non-Thermal Atmospheric Plasma in Cancer Treatment

Eda Gjika

Dissertation Research Committee:

Michael Keidar, A. James Clark Professor of Mechanical & Aerospace Engineering, Dissertation Co-Director

Mary Ann Stepp, Professor of Anatomy and Regenerative Biology and of Ophthalmology, The George Washington University School of Medicine & Health Sciences, Dissertation Co-Director

Jonathan Sherman, Neurosurgeon and Associate Professor of Neurological Surgery, The George Washington University School of Medicine & Health Sciences, Committee Member

Taeyoung Lee, Assistant Professor of Mechanical and Aerospace Engineering, Committee Member

Colin Young, Assistant Professor of Pharmacology and Physiology, The George Washington University School of Medicine & Health Sciences,
Committee Member

© Copyright 2019 by Eda Gjika
All rights reserved

Dedication

This dissertation is dedicated to my parents Irma and Maksi, my brother John and Russell

Thank you for your dedicated partnership for success in my studies

Acknowledgements

This dissertation would not have been possible without the inspiration and support of a number of wonderful people who have continuously contributed to my professional development throughout these past 5 years. I am grateful to all of them. The experiences I have gained at GW are ones that I will forever cherish.

My gratitude first and foremost is extended to my advisor, Dr. Michael Keidar for introducing me to the field of plasma medicine. His kindness, intellectual curiosity, guidance and support have encouraged me to grow professionally and have fundamentally shaped my perspective of research.

I am also deeply grateful to my advisor Dr. Mary Ann Stepp for giving me the opportunity to work in her lab. She is extremely hardworking and persistent, and her mentoring approach throughout the past two and a half years has helped accelerate my intellectual growth and sharpened my curiosity. The collaborative atmosphere in her lab was invaluable for continued progress of this research.

Additional gratitude is extended to my mentors, Ms. Sonali Pal-Ghosh and Dr. Alexey Shashurin for their generosity in sharing their knowledge. Words can never express how grateful I am for the opportunity to have met and learned from such passionate researchers and caring individuals. Dr. Shashurin provided guidance and mentorship from the very beginning of my time in the lab. Two of my first authored publications are the result of his constant support, encouragement and invaluable advice. Through the daily interactions and guidance from Ms. Pal-Ghosh, I have learned a tremendous amount about proper experimental design. Without her patience, guidance, and wisdom, this dissertation work would not have been possible.

I would also like to thank members of my dissertation committee, Dr. Jonathan Sherman, Dr. Colin Young and Dr. Taeyoung Lee for their time in evaluating this dissertation. In particular, I would like to acknowledge Dr. Sherman for his invaluable advice with the plasma-temozolomide experiments.

I am also very grateful to all the collaborators with whom I have interacted. I would like to acknowledge: Dr. Mikhail Pekker, Dr. Alexi Kiss from Dr. Tatiana Efimova's Lab, Dr. Hyak Simonyan from Dr. Colin Young's lab, Dr. Xuan Zhou and Dr. Lijie Grace Zhang at George Washington University. I would also like to extend my gratitude to Dr. Taisen Zhuang and Dr. Jerome Canady at US Medical Innovations and Dr. Navdeep Malik from Dr. Jing Huang's Lab at the NCI. Thank you to Kimberlyn Acklin at the GW Core Flow Cytometry Facility for assisting with the flow cytometric analyses.

A very special thank you also goes to Dr. Gauri Tadvalkar for all her help, encouragement and support with my experiments.

I would also like to thank Ms. Zephra Coles and Ms. Alyssa Pitysingh from the Mechanical and Aerospace Eng. Office and Ms. Brenna Bond in the Anatomy Office for continually providing support and assistance with various matters directly and indirectly related to the successful completion of this work.

Further gratitude is extended to many present and past students and staff at the MPNL lab: Zhitong, Jonathan, Megan, Luis, Xiuqi, Sam, George, Joe, Dayun, Vikas, Xiaoliang, Ram, Kier, Denis, Manish and Carlos for making the environment enjoyable and unforgettable. In particular thank you to Xiaoqian for advising with various experiments and Li for troubleshooting and fixing the plasma device every time I needed help even when it was at the last minute.

A very special thank your goes to my friend Anna Tang who has always been a constant source of encouragement and strength before and during my graduate studies and will continue to be so indefinitely. I deeply appreciate her support in ways too numerous to describe including with parts of the work presented here.

Lastly, I owe the deepest gratitude to my family for all their unconditional love and support. I would like to thank my parents Irma and Maksi, for being a constant source of inspiration and strength, for their dedication to my education, and for instilling in me the virtue of perseverance and commitment to pursue my higher studies. Thank you to my brother John, for an immeasurable level of support in life. Thank you to Russell. Your love, interest in my scientific pursuits and passion for sharing scientific knowledge has been instrumental to my success. To my grandparents and my aunt, thank you for all your wisdom, for all the things said and unsaid, and for your unconditional love.

Abstract

Thermal and Non-Thermal Atmospheric Plasma in Cancer Treatment

Thermal atmospheric plasma technologies such as Argon Plasma Coagulation (APC), have been widely used in medicine to coagulate, cut and ablate tissues. The main effect of these plasmas is created through tissue heating. In contrast, the effect of non-thermal plasma, also referred to as Cold Atmospheric Plasma (CAP), is based on a considerable number of highly reactive chemical species without the presence of heat. Thermal and non-thermal plasmas have a wide range of applications in cancer treatment, from endoscopic APC treatment of early gastric cancer to CAP treatment of glioma. In the past two decades, researchers have focused on further exploring and better understanding the interaction of plasma with living cells and tissue. This dissertation offers insight into the APC-tissue interactions and the CAP-cell interactions.

This study demonstrates that the dielectric properties of biological tissue play a significant role in how the tissue responds to APC treatment. At the tissue level, the APC technique is well-known for thermal non-contact coagulation, with an ability to provide treatment for less accessible regions, and without damage to the tissue. The amount of power applied is one of the key elements for providing a safe and effective treatment. Our results revealed that in the optimal tissue resistance range of 0.8-3.7 kΩ, the majority of the applied power was delivered to the tissue with a small percentage (20-40%) being consumed by the plasma channel. Our findings suggest that surgeons can safely deliver the accurate amount of power by adjusting the power settings based on the expected resistance of the tissue being treated.

Roles of the adaptive properties of CAP, including treatment duration and discharge voltage, in mediating cancer suppression *in vitro,* is an additional topic explored in this dissertation. A proof-of-principle investigation identified the role of discharge voltage in the adjustment of plasma composition and treatment duration in the modification of overall plasma action. The effect of CAP in two cancer cell lines, glioblastoma and breast cancer, was monitored in real-time by observing cell viability. Apoptosis (programmed cell death) was determined to be the likely mechanism initiating a reduction in viable cells via changes to the mitochondrial membrane potential. The findings reveal compelling evidence in support of the important role played by the adaptive properties of CAP, in mediating cancer suppression. The presented discoveries are significant since they will facilitate the future development of a novel adaptive CAP platform which will rely on cell response data collected in real time. Therefore, the optimization of CAP operational parameters via a novel adaptive CAP platform will be essential in providing long-lasting outcomes in cancer therapy.

CAP has also received heightened attention as an alternative therapy due to its ability to impact drug resistant tumors such as gliomas. These tumors have played a significant role in propelling CAP technology to the front lines as a safer alternative compared to more conventional treatment methods such as chemotherapy. This dissertation presents the third investigation of biomedical applications of CAP for sensitizing glioblastoma cells to temozolomide (TMZ). This is also the very first study which explores the role of CAP in cell migration and integrin expression in the presence of TMZ. TMZ concentrations of 10 and 50 μM were evaluated *in vitro* over the course of days with a plasma treatment of 180 seconds. α6 and αv integrins were considered for their roles in

CAP induced cell death, G2/M arrest and decrease in the rate of cell migration. The findings reveal compelling evidence in support of the important role played by CAP in mediating cancer suppression, through direct treatment or by functioning as a drug sensitizing agent.

Table of Contents

Dedication iv

Acknowledgements v

Abstract viii

Chapter 1 Introduction 1

1.1 Background and Motivation 1

1.2 Atmospheric Plasma 1

1.2.1 Thermal and Non-Thermal Atmospheric Plasmas 2

1.3 Plasma Medicine Devices 3

1.4 Cancer Treatment in Plasma Medicine 4

1.5 Objectives and Specific Study Aims 5

1.6 Dissertation Overview and Organization 6

Chapter 2 Plasma Devices 8

2.1 Argon Plasma Electrosurgical System 8

2.2 Cold Plasma Device Set-up 8

Chapter 3 Plasma-Tissue Interactions in Argon Plasma Coagulation: Effects of Power and Tissue Resistance 11

3.1 Introduction 12

3.2 Methods 13

3.2.1 Power and tissue resistance 15

3.2.2 Conductivity Measurements 16

3.3 Results and Discussions 17
3.3.1 Power Produced During Coagulation 17
3.3.2 Equivalent Tissue Resistance and Conductivity 18
3.3.3 Power Distribution 21
3.4 Conclusions 22
Chapter 4 Adaptation of Operational Parameters of Cold Atmospheric Plasma for in Vitro Treatment of Cancer Cells 23
4.1 Introduction 24
4.2 Experimental Section 26
4.2.1 CAP Treatment and Device Operation Parameters 26
4.2.2 Cell Culture 26
4.2.3 Kinetic Study: Cell Viability 26
4.2.4 Hydrogen Peroxide (H_2O_2) Detection 27
4.2.5 Nitrite (NO_2-) Detection 28
4.2.6 Apoptosis: Annexin V and Propidium Iodide Assay 28
4.2.7 Mitochondrial Membrane Potential Assay 29
4.2.8 Nascent Protein Synthesis Assay 30
4.2.9 Image and Statistical Analysis 30
4.3 Results 31
4.3.1 Real Time Monitoring of Cell Response: Treatment Duration and Discharge Voltage 31
4.3.2 Evaluation of H_2O_2 and NO_2^- post CAP Exposure 37
4.3.3 CAP Induced Apoptosis 42

4.3.4 CAP-Induced Mitochondrial Dysfunction 44
4.3.5 CAP in Protein Synthesis 47
4.4 Discussion 50
4.5 Conclusions 54
Chapter 5 Cold Atmospheric Plasma Enhances Sensitivity to Temozolomide in Glioblastoma U87MG Cells 55
5.1 Introduction 55
5.2 Methods 58
5.2.1 CAP Treatment and Device Operation Parameters 58
5.2.2 Reagents and Cell Culture 58
5.2.3 CAP and Temozolomide Treatment 59
5.2.4 Cell Viability Measurement 59
5.2.5 Cell Migration Time-Lapse Studies 60
5.2.6 α6 and αν Immunofluorescent Staining 61
5.2.7 Flow Cytometry and Cell Cycle Analysis 61
5.2.8 Imaging and Statistical Analysis 62
5.3 Results 63
5.3.1 CAP-Enhances TMZ Induced Cell Death 63
5.3.2 Reduced Rate of Cell Migration in CAP-TMZ Treated Cell 67
5.3.3 CAP Treatment Alters Expression of αv and α6 Integrins in TMZ Treated Cells 69
5.3.4 Cell Cycle Changes in G2/M phase 71

5.4 Discussions 73

5.5 Conclusion 75

Chapter 6 Conclusions 76

6.1 Contributions 77

6.2 Future Work 78

Bibliography 80

List of Figures

Figure 2.1 Schematic representation of two plasma devices. 10
Figure 3.1 USMI Electrosurgical system SS-200E. 14
Figure 3.2 Electrical schematics. 15
Figure 3.3 Plasma scalpel directed at the tip of the tissue replica electrode. 16
Figure 3.4 Graph curve of the actual power produced by the ESU. 18
Figure 3.5 Range of equivalent resistance for different types of animal tissue samples. 19
Figure 3.6 The surface of a chicken sample after APC treatment. Scar diameter: 1 cm 21
Figure 3.7 Power distribution in plasma and tissue replica. 22
Figure 4.1 CAP treatment induces a significant reduction in cell viability. 34
Figure 4.2 CAP effect on cell viability varies as a function of discharge voltage. 36
Figure 4.3 Levels of H_2O_2 and NO_2^- in cell culture media after CAP exposure 38
Figure 4.4 CAP generated H_2O_2 becomes metabolically degraded by cancer cells. 40
Figure 4.5 Accumulation of NO_2^- in cancer cells. 42
Figure 4.6 CAP exposure and apoptotic cell death. 44
Figure 4.7 CAP exposure reduces mitochondrial membrane potential in cancer cells 47
Figure 4.8 CAP exposure reduces protein synthesis in cancer cells 49
Figure 4.9 CAP device (a) and adaptive plasma platform (b) 53
Figure 5.1 Inhibition of cell proliferation by Temozolomide. 64
Figure 5.2 CAP sensitizes glioblastoma U87MG cells to temozolomide treatment 66
Figure 5.3 CAP reduces the rate of cell migration in U87MG cells 68
Figure 5.4 CAP mediated αv and α6 integrin expression in TMZ treated cells 71
Figure 5.5 Cell cycle arrest in G2/M phase. 73

Chapter 1

Introduction

1.1 Background and Motivation

"Cancer is a major public health problem worldwide" and one of the leading causes of death among Americans according to the latest available American Cancer Society report published in 2016 [1]. There are still a number of unmet needs that should be addressed even though the mortality rate in the U.S. is among the lowest in the world. In certain cancers, development of resistance to therapy has led to inevitable failure of treatment and increased drug costs [2,3]. While in other cases, successful approaches to treatment have created a number of adverse short- and long- term side effects ranging from discomfort at the treatment site to fatigue while conducting day to day activities [4,5]. Altogether these highlight the necessity for the development of novel treatment methods encompassing new treatment technologies, combined therapies with existent drugs and improved understanding of the efficacy of current treatment modalities. Non-thermal atmospheric plasma-based technologies have emerged in the past two decades as treatment modalities that possess great potential to address some of these needs and assist in immunotherapy [6].

1.2 Atmospheric Plasma

"A radiant matter," this is how Faraday, and later in 1879, a British chemist and physicist Sir William Crooks, described what is referred to as atmospheric plasma in today's modern physics. Plasma, a partially ionized gas known as the fourth state of matter after solid, liquid and gas, was first introduced as a term in l928 by American chemist

Irving Langmuir. According to records, Langmuir decided to use this term because the compositions of the strongly ionized gas reminded him of blood plasma [7–9].

Plasma is formed by applying energy across a gas which leads to an increase in the number of collisions between individual constituents, causing their energies to increase further and prompt an ionization and dissociation process. This results in a state of matter comprised of a wealth of fascinating chemistry including: ions, free electrons, photons and radicals [10]. Most of the visible matter in the universe is in fact in a plasma state; this includes the stars, solar corona and the sun. Plasma can also be found on earth in the form of flame and lighting and it can be man-made in the form of neon signs and spark plugs. Man-made plasma has been exploited in wide range of applications including surface modifications, environmental remediation, biotechnology and medicine.

1.2.1 Thermal and Non-Thermal Atmospheric Plasmas

In medicine, plasma is utilized in thermal and non-thermal forms by employing gases such as argon and helium. In both cases it is created by the application of an electric field across a gas, which causes the electrons to break free from the atoms. Being lighter than ions, electrons receive the applied energy first, and consequently their temperature rises several thousand degrees before their surrounding environment. Thermal plasma is formed in the case of successful heat transfer from electrons to heavy particles (ions and neutrals). This creates what is known as a state of thermal equilibrium, where the temperature of heavy particles reaches almost the same order of magnitude as that of the electrons. In contrast, non-thermal plasma can be achieved by preventing the transfer of heat, creating a state where the temperature of the electrons continues to remain far greater

than that of the heavy particles, resulting in a near ambient temperature plasma (NTP). This non-equilibrium plasma is also referred to as cold atmospheric plasma (CAP) because the temperature at the point of application does not exceed 40°C [7,11–13]**.** Several methods can be utilized to achieve a low temperature plasma including altering the amount of time over which the electric field is applied across a gas [14].

1.3 Plasma Medicine Devices

Plasma devices have been adapted and improved over time to fit the needs of the plasma medicine field. Plasma devices can be classified as direct or indirect according to the mechanism used for generating them, and within these classes they can be further categorized as thermal and non-thermal. Direct plasma sources generate plasma between two electrodes with the living tissue serving as one of the electrodes [15]. APC (in thermal plasma) and Dielectric Barrier Discharge plasma (DBD) (in non-thermal plasma) are typical examples of direct plasma sources. [13,16]. Plasma generated via DBD is created by applying high voltage short duration pulses between two electrodes. The treatment site serves as the second electrode. Whereas the first electrode is insulated with a dielectric material to prevent current buildup that may occur between the two electrodes [16–21]**.** The FE-DBD developed by researchers at Drexel University is a typical example of this [14]. In the indirect approach, plasma is generated remotely between two electrodes and it utilizes gas flow to be transported to the targeted treatment area of the biological tissue. A typical example of plasma jet generated with an indirect approach include the non-thermal plasma pencil developed by researchers at Old Dominion University, the kINPen

developed by investigators at the Leibniz-Institute for Plasma Science and Technology, INP Greifswald, Germany [22–24]

1.4 Cancer Treatment in Plasma Medicine

Plasma medicine has become one of the fastest growing fields connecting medicine with physics, chemistry, engineering and biology. The first application of plasma in healthcare dates back to the 1850s when Siemens generated ozone via dielectric barrier discharge for cleaning water from biological contaminants [13,25]. Other applications that followed involved the application of plasma in electrosurgery for coagulating and devitalizing tissue. An example of this is Argon Plasma Coagulation (APC), first used in surgery in the late 1970 and adapted for flexible endoscopy use in the 1990 [26]. APC continues to be a very common technique employed in electrosurgery with many applications, including tumor debulking, ablation of vascular malformations, and coagulation of peptic ulcer bleeding sites [27–31]. In the early 2000s interest started to shift to the applications of cold plasma in cancer treatment. In 2004 Eva Stoffels and her group were the very first to report on the interactions of plasma with mammalian cells. The group showed that following plasma treatment, fibroblast and vascular cells detached from the surface of a cell culture dish in a time dependent manner. The detachment occurred in the area of plasma impact and was followed by a decreased cell viability resulting from applying plasma at higher powers. Although their results were not obtained in cancer cells, they were significant because they were the first ones to establish the basic effects of cold plasma on mammalian cells [32,33]. Studies that followed corroborated Stoffels' findings *in vitro* in several types of cancers including: melanoma, cervical cancer, breast cancer,

lung cancers and glioblastoma [34–42]. Few years later, some of these findings were also investigated *in vivo*. The first *in vivo* investigation in mice was reported in 2010 by Marc Vandamme and his co-workers. The study examined the role of CAP in the treatment of glioblastoma. In 2011 Michael Keidar and co-workers examined the effect of CAP treatment in a melanoma mouse model and a heterotopic human bladder cancer xenograft model. In both investigations, researchers found that CAP treatment instigated a significant reduction in tumor volume and increased survival time [43,44]. These observations were later supported by additional *in vivo* studies in different cancer types [34,45]. After over a decade of CAP investigation in oncology, most recent studies are primarily concerned with elucidating cellular mechanisms that mediate cell response to CAP treatment with a particular emphasis on the role played by CAP generated reactive oxygen and nitrogen species [46].

1.5 Objectives and Specific Study Aims

Thermal and non-thermal plasma technologies are being explored for medical research in the rapidly growing field of plasma medicine. The objective of this study is to: 1) better understand the plasma-tissue interactions in APC; 2) emphasize the importance of the CAP operational parameters by comparing the effect of CAP in different cancers and; 3) evaluate a new application of CAP as a potential method for sensitizing cells to drug treatment.

Specific Aim 1: Evaluate the role of biological tissue in the operation of an APC device during treatment.

Sub Aim 1.1: Determine the anticipated tissue resistance under which the device operates in optimal conditions.

Sub Aim 1.2: Evaluate the correlation between tissue conductivity and applied power. More specifically investigate what percentage of the applied power is delivered to the treatment site.

Specific Aim 2: Investigate the role of the adaptive properties of CAP, treatment duration and discharge voltage, in mediating cancer suppression *in vitro.*

Sub Aim 2.1: Identify methods for monitoring cell response in real time so that plasma operational parameters can be adjusted to tailor CAP therapy to various cancers.

Sub Aim 2.2: Elucidate on the importance of adapting CAP operational parameter by comparing responses to plasma treatment in two different types of cancers *in vitro*.

Sub Aim 2.3: Investigate the effect of CAP on several cellular processes that are linked to apoptosis.

Specific Aim 3: Determine the role of CAP in cancer cell sensitization to chemotherapeutic drug temozolomide (TMZ).

Sub Aim 3.1: Determine if plasma can improve TMZ treatment outcomes by more significantly increasing cell death in comparison to plasma and TMZ as standalone therapies.

Sub Aim 3.2: Evaluate cell response to CAP and TMZ in the context of cell migration, integrin expression and cell cycle arrest.

1.6 Dissertation Overview and Organization

This dissertation is focused on the biomedical applications of thermal and non-thermal plasma. The findings presented are organized in five chapters. Chapter 1 gives an

introduction of plasma and presents the objectives and specific aims of this dissertation. Chapter 2 describes the plasma devices utilized in this study. Chapters 3 - 5 present original experimental findings. Results described in chapter 3 and 4 have been published in peer reviewed journals. Experimental results presented in chapter 5 are been utilized for the preparation of a manuscript. Chapter 3 investigated the thermal plasma - biological tissue interaction in APC. More specifically it investigates the role of biological tissue properties (i.e. resistance and conductivity) during APC treatment. This chapter also inadvertently introduces a method for testing the accuracy with which plasma devices operate and it does so by comparing the power setting with the measured delivered power. The results presented in Chapters 4 and 5 aim to investigate the application of cold plasma in cancer treatment and are carried out *in vitro* in breast cancer and glioblastoma cell lines. Chapter 4 validates a method for monitoring cell responses in real time. This method will be utilized in the near future for the development of a novel plasma platform. Here, microscopy and flow cytometry techniques are utilized to characterize how changes in CAP treatment parameters influence cell response. Chapter 5 seeks to explore a new application of plasma in cancer treatment, that of sensitizing cancer cells to TMZ. The positive effect of plasma when combined with Temozolomide (TMZ) is considered as a function of cell migration and integrin expression. Chapter 6 concludes the dissertation by summarizing the results presented in the previous chapters.

Chapter 2

Plasma Devices

2.1 Argon Plasma Electrosurgical System

The findings presented in Chapter 3 were acquired from experiments conducted with the SS-200 E/Argon - 2 electrosurgical system developed by US Medical Innovation. The device was operated in coagulation mode [47,48]. A schematic representation of a typical APC setup is shown in Figure 3.1(a).

2.2 Cold Plasma Device Set-up

Two cold plasma devices were built at the Micropropulsion and Nanotechnology Laboratory (MPNL) of Dr. Michael Keidar at The George Washington University (Washington, DC). The first setup, a prototype of the original plasma gun created by Dr. Alexey Shashurin and assembled by Dr. Olga Volotskova, was utilized for the experiments in Chapter 4 [49,50]. The second device is an improved version of the first device and it contains a function generator instead of a LM555 circuit. This device was utilized for the experiments in Chapter 5 and was built by Li Lin, an MpNL Ph.D. student [51,52]. A schematic representation of a typical CAP jet is shown in Figure 2.1 (b).

The CAP device utilized in chapter 4 consisted of a helium gas supply, DC voltage supply, circuit box, and plasma head. The gas supply inlet of the devices is connected to flowmeter (Cole-Parmer) that can connect to a helium tank. The utilized DC voltage supply is from Insteak (SPS-606 60V/6A). The circuit box consists of three major components: 1) a capacitor used to prevent undesirable negative feedback waveforms (high-voltage surges),

2) a transistor which acts as a switch between the DC power supply and the plasma jet and 3) a LM555 timer circuit used to drive the transistor. The LM555 timer is connected in a stable operation mode and therefore its frequency is independent of voltage supply. In contrast, the CAP device utilized in chapter 5 contained all the above elements with the exception of the LM555 timer circuit. In the new and improved device, the LM555 timer circuit is replaced with a function generator and a new 3D printed housing unit holds the device.

The plasma head is the main active part of the device where the CAP jet is generated. The plasma head is composed of a cylindrical shaped glass tube which serves as the CAP jet nozzle and it is connected with two high-voltage electrodes connected with the flyback transformer. The first high-voltage electrode is located inside the glass tube and it is isolated from direct contact with plasma by ceramic. The second electrode which serves as ground, is copped based and it is wrapped around the outside of the glass nozzle in a ring shape.

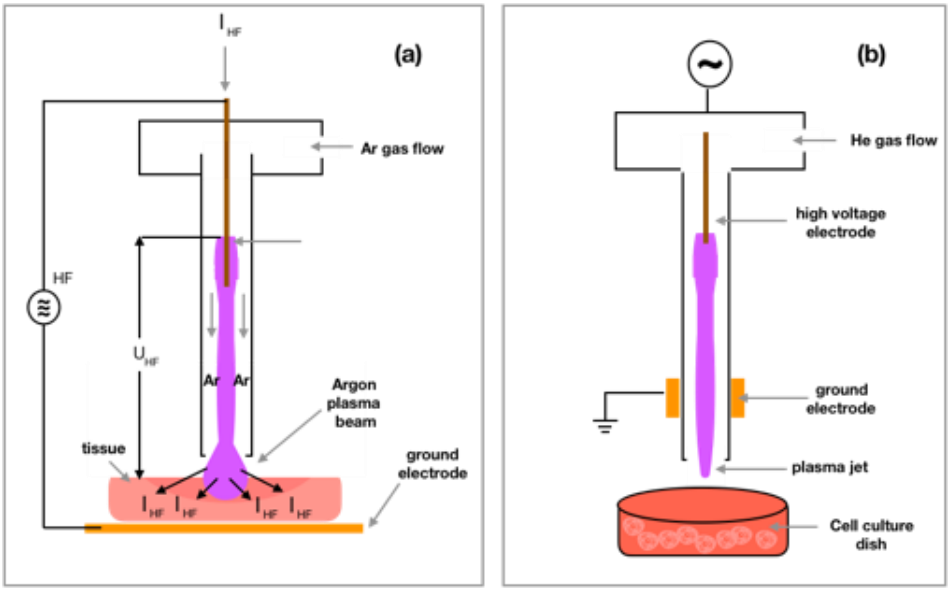

Figure 2.1 Schematic representation of two plasma devices. (a) Schematic representation of a typical APC setup with argon flowing through a tube containing the electrode wire. (b) Schematic representation of the cold atmospheric pressure plasma jet configuration.

PUBLISHED ARTICLE

Chapter 3

Plasma-Tissue Interactions in Argon Plasma Coagulation: Effects of Power and Tissue Resistance

ABSTRACT

The coagulation properties of the Argon Plasma Coagulation (APC) technique have tremendous potential due to a wide range of endoscopic applications. Although there are several studies that explore the endoscopic application aspect of this technique, there has been no research devoted to the investigation of relevant argon plasma properties during coagulation. We investigated the role of power in the interactions between plasma and biological tissue and reported on the dielectric properties of APC treated samples. The data revealed that at a resistance of 1 $k\Omega$ the actual power observed was within 10 – 15% of the input power of the system and, the typical resistance for animal samples was in the range of 0.8 – 3.7 $k\Omega$. The data also suggested that the amount of power applied could be adjusted according to the expected tissue resistance range. Additionally, it was determined that the burned surface caused by the APC treatment was on average 2 – 3 times less conductive than the untreated surface. The data also revealed that 60 – 80% of the power produced by the electrosurgical generator was delivered into the biological tissue and the plasma channel consumed the remaining 20 – 40%. This study establishes a guide for the investigation of optimal argon thermal plasma properties for biological tissue application.

3.1 Introduction

Argon Plasma Coagulation (APC), first used in surgery in the late 1970s, has rapidly become one of the most common techniques employed in electrosurgery. APC offers many potential applications, including tumor debulking, ablation of vascular malformations, and coagulation of peptic ulcer bleeding sites [27–31]. Some of the most common gastrointestinal (GI) diseases treated by APC include: radiation proctitis, Barrett's esophagus and gastric antral vascular ectasia [GAVE] [53–60]. APC is a preferable treatment method since it conducts electrical current in a non-contact manner. The ability to ablate tissue without direct contact is beneficial as it may mitigate the risk of bleeding at the targeted site and the surrounding tissue. The scalpel is positioned 2 – 6 mm from the treatment site and thermal heating is achieved by high purity ionized argon gas. The produced heat denatures the proteins and evaporates the intra- and extracellular water, resulting in tissue destruction and coagulation [28,53,61]. The tissue's response to thermal heating is directly dependent on the amount of power applied. The applied power ranges from 20 – 90 Watts based on the type of treatment [62–65]. While the applied power used for treatment is under investigation, little is known about the physical properties of plasma employed and the plasma-tissue interaction during coagulation. Basic plasma parameters, such as argon plasma density and electrical conductivity using the Rayleigh Microwave Scattering have been previously reported by our group [61]. Plasma density was determined to be in the range of $(7.5 – 9.5) \cdot 10^{15} cm^{-3}$ and the electrical conductivity was at (1 – 2) $Ohm^{-1}\, cm^{-1}$. In this paper we present data of plasma-tissue interactions during APC treatment, which was obtained by determining the accuracy of the power produced by the electrosurgical unit based on tissue resistance. To our knowledge, these plasma –

tissue interactions have never been investigated before. We also elucidate the power distribution between plasma and tissue, and report on the conductivity of APC treated samples. A better understanding of these interactions would offer more insight into the properties of argon plasma and the amount of power required for an effective treatment.

3.2 Methods

The experiments were conducted using the electrosurgical system SS-200E/Argon 2 (ESU) in combination with the electrosurgical scalpel by US Medical Innovations, LLC, shown in Figure 3.1. Since power settings and argon gas flow rates vary depending on the type of treatment, we selected conditions representative of clinical uses. The SS-200E/Argon-2 was operated in coagulation mode at 40, 60 and 80 Watts with a 3 LPM flow rate of argon. The patient port of the ESU was grounded in all experiments. Several raw animal tissue samples were purchased frozen from a local food store and were thawed to 18 – 21℃ before being used for the experiment. The scalpel was positioned between 2 – 6 mm away from the biological tissue for 2-5 seconds to achieve stable and continuous flow of argon plasma. The depth of the burn injury was neither considered nor investigated in this study.

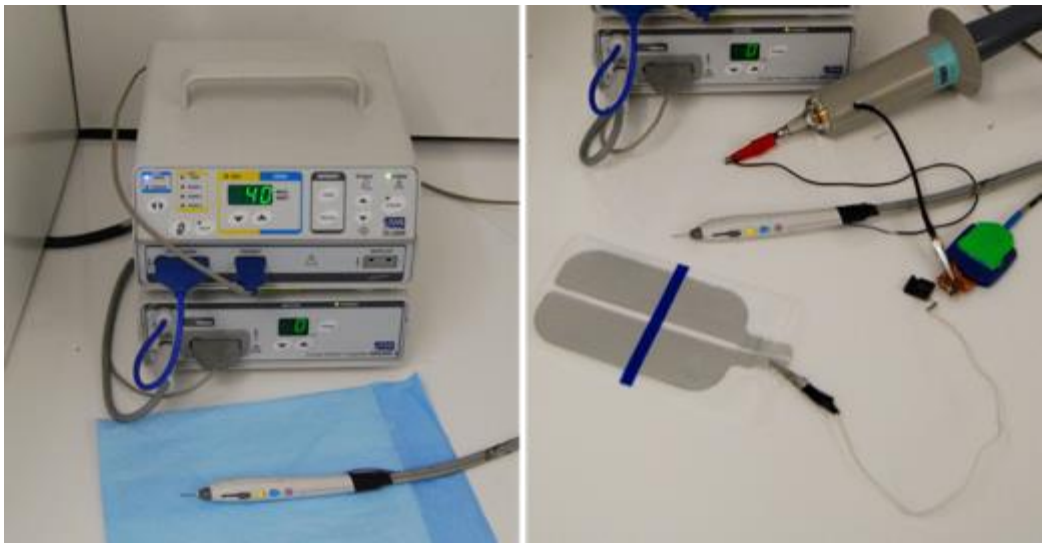

Figure 3.1 USMI Electrosurgical system SS-200E and the argon delivery unit Argon2 coupled to the Canady Vieira hybrid Plasma Scalpel from US Medical Innovations, LLC; Experimental components: Patient port from the ESU connected to a non-inductive thin film resistor and USMI patient pad, high voltage probe, and USMI plasma scalpel.

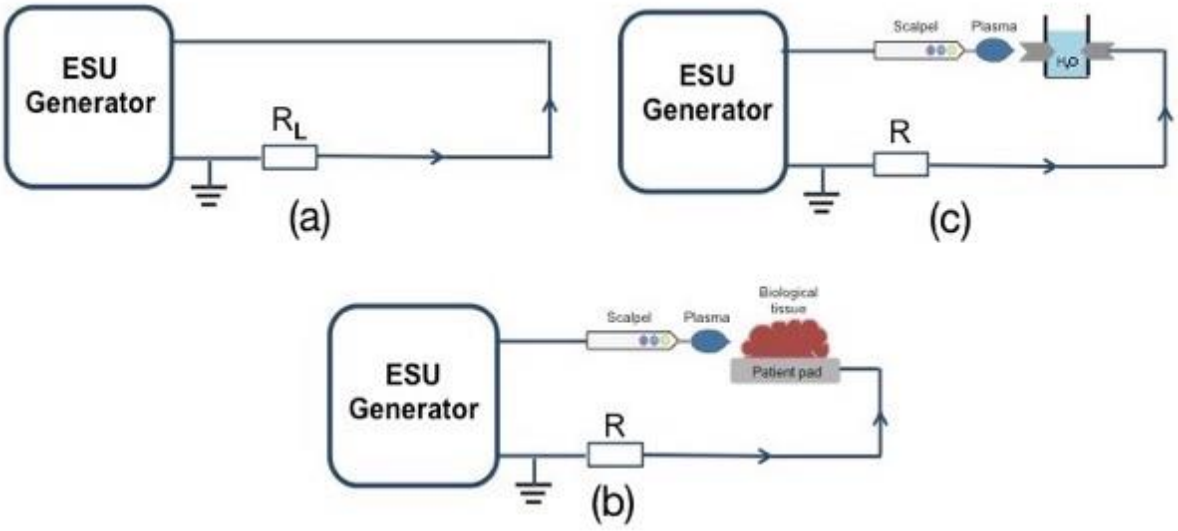

Figure 3.2 Electrical schematics: (a) actual power produced by the ESU during coagulation across RL of 0.2, 0.5, 1, 5, 10, 15, 20, 30 and 40 **kΩ**, (b) equivalent tissue resistance experimental set-up, and (c) power distribution experiment with a deionized water sample as tissue replica.

3.2.1 Power and tissue resistance

The power produced by the ESU generator across the RL was measured. Various non- inductive thin film shunt resistors (0.2, 0.5, 1, 5, 10, 15,20 30 and 40 kΩ) were placed in series to determine the current produced by the circuit. The resistors were connected directly to the high voltage generator and the patient port of the ESU as shown in Figure 3.2 (a). The voltage produced by the ESU was measured with the high voltage probe shown in Figure 3.1. The experiment was conducted at the power settings of 40, 60 and 80 Watts and the actual power produced was calculated from

$$P = \left(\frac{U^2}{R_L}\right)$$

where U is the measured voltage produced by the scalpel and (RL) = 0.2, 0.5, 1, 5, 10, 15, 20, 30 and 40 kΩ.

The ranges of equivalent resistance for the biological samples during APC treatments were determined following observations from the first experiment. Samples containing different density levels of muscle and connective tissue were selected. Raw animal tissue samples from pork belly, cow pectoral, lamb liver, chicken liver and chicken leg were tested as shown in Figure 3.2 (b). A 10 Ω non-inductive thin film shunt resistor was used to determine the current generated in the circuit. The distance between the plasma scalpel and the tissue was measured and kept between 2 – 6 mm.

Additionally, the power distribution between plasma and tissue was investigated following the schematic shown in Figure 3.2(c). The replica, comprised of two metal electrodes separated by a deionized water gap, was used for testing (Figure 3.3). Voltages were measured on both sides of the plasma channel and the current was calculated using Ohm's law and a 10 **Ω** shunt resistor. Measurements were taken at a 3, 4.5, and 6 mm distance between the tip of the plasma scalpel and the tip of the replica electrode. The distances selected were within the acceptable range for maintaining a stable plasma flow. The power delivered to the plasma and tissue replica was determined by numerically integrating the instantaneous powers.

Figure 3.3 Plasma scalpel directed at the tip of the tissue replica electrode.

3.2.2 Conductivity Measurements

A four-point probe method was used to determine the resistance of the fresh chicken samples. A set of voltage electrodes spaced 1 – 2 cm apart, was placed in the sample between the two current electrodes. A 300 Ω shunt resistor was used to determine the

current produced by the power source. The AC power source was set to 5 volts. The specific conductance between the inner electrodes was determined by measuring the current across the resistor as well as the voltage drop across the inner electrodes that were embedded in the sample. The two-point probe method was used to determine the relative conductivity between the surface of the untreated and treated tissue.

3.3 Results and Discussions

3.3.1 Power Produced During Coagulation

Figure 3.4 compares the actual power produced by the ESU generator to the load resistance at the power settings of 40, 60 and 80 Watt. It was observed that as the resistance approached 1 kΩ, the applied and set powers were similar. The actual power produced by the ESU generator ranged within 10-15% from the power setting for all tested conditions. The gray bar in Figure 3.4 indicates this trend and shows that the resistance of the biological tissue is expected to be close to the 1 kΩ range during APC treatment. The data also revealed that the power decreased and neared zero when the load resistance (R_L) was greater than 10 kΩ. Figure 3.4 reveals that for resistances greater than 1 kΩ the instrument was able to produce a power smaller than the one of the power setting. If the resistance of the tissue were to be substantially smaller than 1 kΩ, the applied power may lead to extensive tissue injury. The difference in power can be attributed to the resistance of the instrument since each power setting corresponds to an average resistance, which can be limiting. The user cannot modify this characteristic of the APC system, which could prove to be a major safety concern. The data suggested that the power setting could be adjusted based on the expected resistance of the tissue.

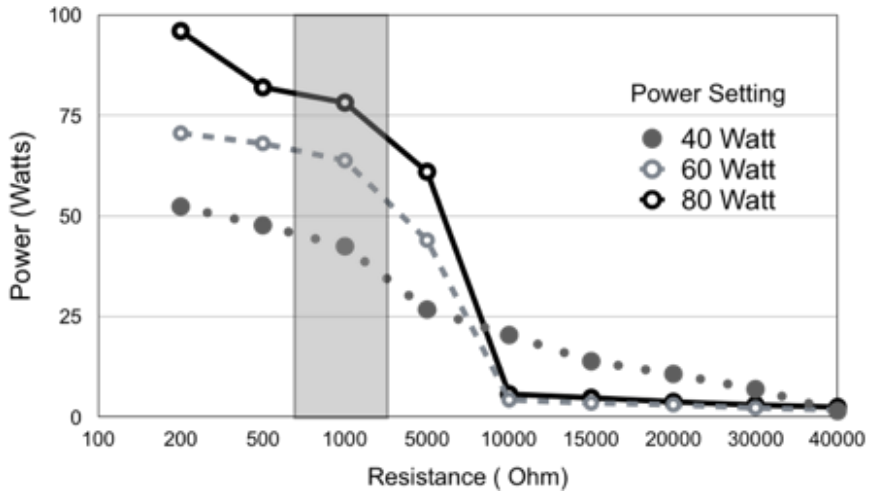

Figure 3.4 Graph curve of the actual power produced by the ESU against the load resistance (RL of 0.2, 0.5, 1, 5, 10, 15, 20, 30 and 40 **kΩ**) for 40, 60, and 80 Watts of applied power.

3.3.2 Equivalent Tissue Resistance and Conductivity

Figure 3.5 compares the resistance of five animal samples during APC treatment. The equivalent resistance for each biological sample was calculated by dividing the measured voltage by the discharge current for the time periods of the plasma discharge. The observed equivalent resistance (R_{eq}) ranged from 0.8 – 3.7 **kΩ**. We anticipated for human and animal tissue to have a similar resistance range. To confirm these findings, the conductivity of animal tissue was measured and compared with the conductivity range for human tissue that was previously reported in literature.

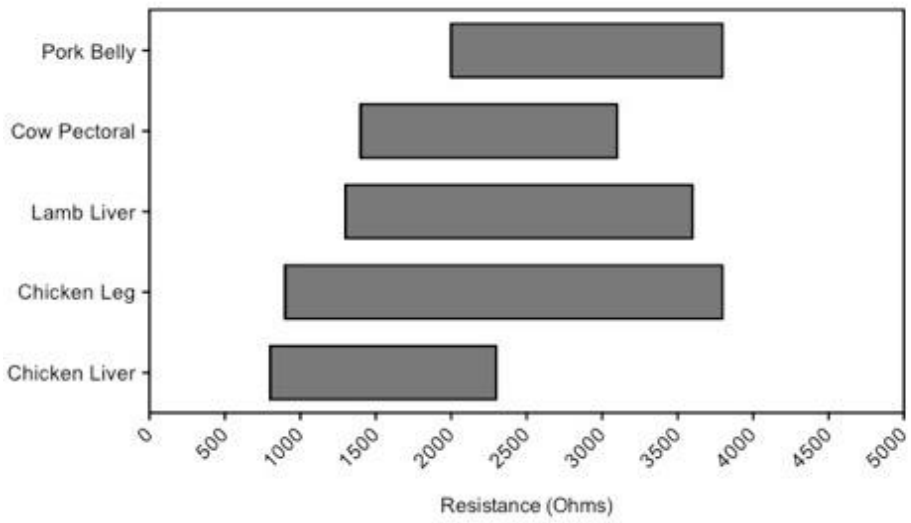

Figure 3.5 Range of equivalent resistance for different types of animal tissue samples.

The reported conductivity for different human and animal tissue encompasses a large range (0.02 – 1.4 S/m), in part due to the different methods used for carrying out the measurements. For example, Bodakian and Hart reported low values for the conductivity of chicken samples varying from 0.02 – 0.025 S/m, which may have resulted from using the two-point probe method [66]. With the four-point probe, we observed that the contact voltage drop at the probe-tissue interface was higher than the contact voltage drop of the tissue. The two-point method does not account for this voltage drop, therefore the literature reported values for conductivity might be underestimated.

The conductivity of our samples ranged from 0.2 – 0.6 S/m. This range was in accordance with the values reported in the literature for both healthy and tumor tissue [66–75]. Based on these findings we established that during APC treatment the resistance of human tissue is similar to that of animal tissue. Figure 3.6 shows the surface of the chicken sample after treatment with argon plasma. The electrical conductivity of the cauterized samples was determined using relative measurements of the untreated and cauterized surfaces. We

established a coefficient (α) to characterize the change in conductivity. We established a coefficient (α) to characterize the change in conductivity.

$$\alpha = \left(\frac{\sigma_c}{\sigma_{nc}} \right)$$

(1)

where (σ_c) and (σ_{nc}) are respectively the conductivities in the cauterized area and non-cauterized areas of the living tissue. The ratio $\left(\frac{\sigma_c}{\sigma_{nc}} \right)$ was determined using a current probe. The probe, comprised of two conducting electrodes at 3 mm apart, provided stable contact with the tissue. The voltage difference between the probe wires was kept at 1 volt. Numerous current measurements were recorded to determine the average currents in the cauterized (i_c) and the non-cauterized areas (i_{nc}). The α coefficient was determined as follows:

$$\alpha = \left(\frac{\sigma_c}{\sigma_{nc}} \right) = \left(\frac{i_c}{i_{nc}} \right)$$

(2)

The range for the (α) coefficient was calculated to be from 0.3 – 0.5, which indicated that the cauterized area was less conductive than the non-cauterized one. This result was in support of the limited depth of injury that the APC treatment offers.

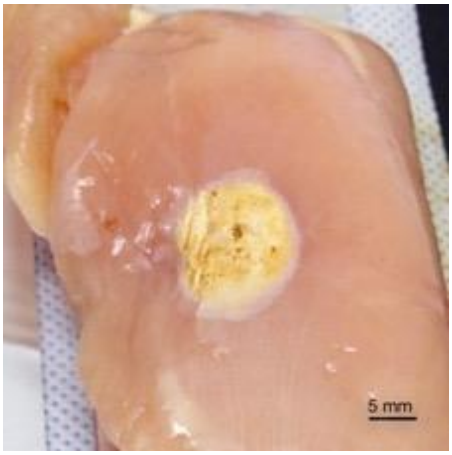

Figure 3.6 The surface of a chicken sample after APC treatment. Scar diameter: 1 cm

3.3.3 Power Distribution

The power distribution between the tissue and plasma is shown in Figure 3.7. The experiment was conducted using a tissue replica as shown in Figure 3.2 (c). In a previous study, the waveforms of the discharge voltage and current generated for the chicken samples were compared with that of the deionized water replica. It was determined that their electrical discharge was similar [76] and therefore the replica was used for this testing. It was observed that 60 – 80% of the power produced by the ESU was delivered to the tissue, while the rest was consumed for the production of the plasma. A portion of the power applied to the plasma channel was independent of the size of the gap created between the replica and the tip of the plasma scalpel in Figure 3.3. These findings are significant since, to our knowledge, there are no other studies that report of the power distribution of APC systems during treatment.

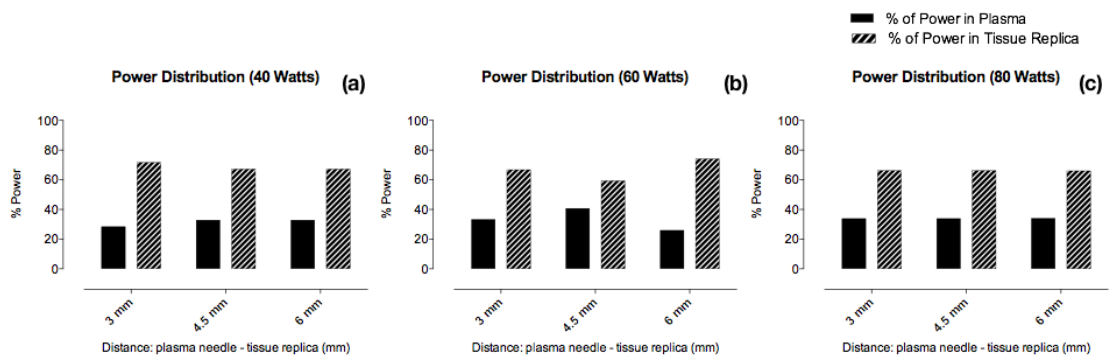

Figure 3.7 Power distribution in plasma and tissue replica for power settings of 40, 60, and 80 Watt.

3.4 Conclusions

Sample conductivity, resistance and the amount of applied power determine the type of burn created by APC treatment. A burned surface caused from the brief exposure to argon plasma was determined to be 2 – 3 times less conductive in comparison to an untreated surface. The amount of power delivered to the treatment site was found to be dependent on the resistance of the tissue. If the resistance of the target tissue were to be outside the range of 0.8 – 3.7 kΩ, an inconsistent amount of power would be delivered, resulting in ineffective treatment or extensive thermal damage. This study suggests that surgeons can adjust the power setting based on the expected resistance of the tissue being treated. When in the optimal resistance range, the majority of the applied power will be delivered to the target area, though a small percentage of it will be consumed by the plasma channel. Therefore, it is important to investigate APC units from different companies as the accuracy of the delivered power may slightly differ among them. Inaccuracies in delivered power may greatly affect the treatment of many diseases.

PUBLISEHD ARTICLE

Chapter 4

Adaptation of Operational Parameters of Cold Atmospheric Plasma for in Vitro Treatment of Cancer Cells

ABSTRACT

Cold atmospheric plasma (CAP), an ionized gas operated at near ambient temperature has been introduced as a new therapeutic opportunity for treating cancers. The effectiveness of the therapy has been linked to CAP generated reactive oxygen and nitrogen species such as hydrogen peroxide and nitrite. In this study, we monitor in real time cancer cell response to CAP over the course of 48 hours. The results demonstrate a correlation between cell viability, exposure time (30, 60, 90, 180-s) and discharge voltage (3.16 and 3.71 kV) while stressing the likely therapeutic role of plasma-generated reactive species. A 30-60 second increase in CAP exposure time and/or a discharge voltage adjustment from 3.16 to 3.71 kV, is consistently accompanied with a significant reduction in cell viability. Comparably, levels of hydrogen peroxide and nitrite vary as a function of voltage with elevated levels detected at the highest tested voltage condition of 3.71 kV. CAP ultimately initiates a reduction in cell viability and triggers apoptosis via damage to the mitochondrial membrane while also deregulating protein synthesis. The findings presented in this study, are discussed in the context of facilitating the development of an adaptive CAP platform which could improve treatment outcomes.

Keywords: Non-thermal atmospheric plasma, reactive oxygen species, reactive nitrogen

species, discharge voltage, treatment duration, apoptosis, mitochondrial membrane potential, protein synthesis.

4.1 Introduction

Non-thermal atmospheric plasma, also referred to as cold atmospheric plasma (CAP), has emerged in the past two decades as a promising cancer therapy [77–79]. CAP is formed by applying a high electric field across a gas. This accelerates electrons into nearby atoms and molecules leading to a cascade effect of ionization, excitation and dissociation processes, ultimately creating a unique environment of positive and negative charges, UV radiation, reactive species and neutral molecules[80]. CAP therapeutic effects have been linked to high concentrations of reactive oxygen and nitrogen species (RONS), including: atomic nitrogen [81] and oxygen [82,83], hydroxyl (OH) [84], singlet delta oxygen (SDO) [85], superoxide [86], and nitric oxide (NO) [87,88]. These active species have been extensively reported as key mediators of oxidative damage and cancer cell death during plasma treatment [39,89,90]. Furthermore, the interaction of these species with cell culture media has played an important role in treatment outcomes. In a previous study it was shown that the efficacy of CAP treatment can be regulated by the concentration of FBS in media [91].

Recent studies have introduced CAP as a selective therapy with a high affinity for triggering death in cancer cells while leaving normal cells unharmed and with no specificity to any type of cancer [40,80,86]. Several investigators have reported the successful application of CAP for in vitro treatment of approximately 20 cancer types including neuroblastoma [92], pancreatic carcinoma [93,94], melanoma [95–97] cervical carcinoma

[98][99], lung carcinoma [92][100], head and neck carcinoma [92], and breast cancer [100][101].

Results from previous studies reveal that different types of cancers exhibit different responses when exposed to the same CAP treatment conditions. Therefore, it is essential to identify methods for monitoring cell response in real time so that plasma operational parameters can be adjusted to tailor CAP therapy to cancers at various stages. An understanding of the role of CAP operational parameters is significant since they control the chemical composition of plasma and thereby the quantity of RONS delivered by it.

Here, we conduct a proof-of-principle investigation to identify the role of two CAP operational parameters: 1) discharge voltage in the adjustment of plasma composition and 2) treatment duration in the modification of overall plasma action. We monitor the effects of CAP in breast cancer and glioblastoma cell lines in real-time by observing cell viability and levels of exogenous and endogenous H_2O_2 and NO_2^- within each cell culture. Programed cell death (apoptosis) is investigated as a likely mechanism initiating a reduction in viable cells via changes to the mitochondrial membrane potential [102]. Furthermore, our study presents the first experimental evidence concerning the impact of CAP in protein synthesis – responsible for disruption in cancer growth and development [103]. The presented work is important since it addresses the significance of monitoring cell response in real time, the role of CAP discharge voltage and exposure time as key factors in the effectiveness of CAP therapy. The operational CAP properties are further discussed for their potential application in the development of an adaptive CAP platform. The novel platform could enhance selective destruction of cancer cells independent of cancer type or CAP treatment condition.

4.2 Experimental Section

4.2.1 CAP Treatment and Device Operation Parameters

The CAP device was manufactured at the Micro-propulsion and Nanotechnology Laboratory of the George Washington University. The device was operated at a frequency of 13kHz with a helium flow rate of 4 - 5 L/min. The helium plasma jet was generated via the dielectric barrier discharge. The spot size of the plasma jet when in contact with liquid media had a diameter of about 10 mm. The distance between the plasma jet outlet and the surface of the cell culture medium was fixed at 2 cm. The device was operated in the discharge voltage range of 3 – 6 kV with results presented at 3.16 and 3.71 kV. Plasma treatment was performed in a direct method with cells treated in culture medium and the CAP effect was quantified for different post exposure time points (0 minutes – 48 hour).

4.2.2 Cell Culture

Human cancer cell lines, U87 (glioblastoma) and MDA-MB-231 (breast adenocarcinoma) were obtained from the American Type Culture Collection (ATCC) (Manassas, VA). Epithelial cell lines were cultured in Dulbecco's Modified Eagle Medium (DMEM) (Life Technologies) supplemented with 10% (v/v) fetal bovine serum (ThermoFisher) and 1% (v/v) Penicillin and Streptomycin (Life Technologies). Cell cultures were maintained at 37°C in a humidified incubator containing 5% (v/v) CO_2.

4.2.3 Kinetic Study: Cell Viability

CAP-induced cell death was investigated by RealTime-Glo MT Cell Viability Assay (Cat. no. G9711, Promega) with a continuous read method for up to 48 hours post

CAP exposure. The assay measured cell metabolic activity which served as a proxy for cell viability. Adherent cells were plated in tissue culture grade white-walled 96-well plates at a density of 5000 cells in 100 μL of DMEM media per well. Cells were incubated overnight at 37°C in a humidified incubator. Subsequently at 60% confluency, culture media was replaced with 50 μL of fresh media to remove any unbound cells. The 2X RealTime-Glo solution was prepared following manufacturer's protocol by diluting 2 μL of MT Cell Viability Substrate and 2 μL of NanoLuc Enzyme in 996 μL of DMEM. Once prepared, 50 uL of the 2X solution was added to cells in 50 uL of culture medium for a final volume of 100 uL per well. The plates were incubated overnight to allow complete incorporation of the reagents. Following manufacturer's protocol, the cell culture media was not replaced prior to CAP treatment since this would cause the NanoLuc enzyme in the media to be removed and the assay to be invalid. Cells were treated with CAP for 30, 60, 90 and 180 seconds at 3.16 or 3.71 kV. Luminescence was measured with a Thermo Viroskan LUX microplate reader at 37°C immediately upon CAP treatment for every 10 minutes up to 1 hour and at 6, 12, 24 and 48 hours. Luminescence intensities of the CAP treated condition were normalized to untreated CAP sample (control). Each condition was performed in triplicate and the experiment was repeated three times.

4.2.4 Hydrogen Peroxide (H_2O_2) Detection

Extracellular H_2O_2 present in cell culture after CAP treatment was detected with a Fluorimetric Hydrogen Peroxide Assay (Cat. no. MAK165, Sigma-Aldrich). Cells were seeded in 96-well culture plates at a density of 5000 cells in 100 µL of DMEM media and allowed to adhere overnight. The cell culture media was replaced with 100 µL of fresh

media prior to treatment with CAP. At least 50 µL of the culture media from treated cells were transferred per well into a black-walled 96-well plate and the assay was conducted following manufacturer's protocol. Fluorescence intensity was quantified at excitation/emission wavelengths of 540/590 nm respectively with readings at 0 - 60 min and 6, 12, 24, 48 hours post treatment at 3.16 and 3.71 kV with a Synergy H1 Hybrid Multi-Mode microplate reader. The mean of the optical density values was compared to a standard curve and results were expressed in units of µM.

4.2.5 Nitrite (NO_2^-) Detection

The concentration of nitrite (NO_2^-), a stable downstream product of nitric oxide (NO) was detected with Griess Reagent Assay (Cat. no. G2930, Promega) according to manufacturer's instructions. Cells were seeded in 96-well culture plates at a density of 5000 cells in 100 µL of DMEM media and allowed to adhere overnight. The culture media was replaced with 100 µL of fresh media prior to CAP treatment. After incubation for 0-48 hours, 50 µL of the treated suspensions were transferred per well into a clear-walled 96-well plate and the assay was conducted following manufacturer's protocol. Absorption was measured with a microplate reader at 560 nm for the following time points: 0-60 min, 6, 12, 24 and 48 hours post CAP exposure. The results of a standard curve were utilized to translate the optical density values into nitrite concentration expressed in µM.

4.2.6 Apoptosis: Annexin V and Propidium Iodide Assay

Annexin V assay was performed with a FITC Annexin V Apoptosis Detection Kit I (Cat. no. 556547, BD Biosciences) as recommended by the manufacturer. Cells cultured

in 24-well plates (25,000 cells per well) were treated with plasma for 60 seconds. At 0, 20, 40, 60 minutes and 6, 12, 24 and 48 hours post treatment, the cells in the supernatants were collected by centrifugation. Adherent cells were harvested by Accutase (Innovative Cell Technologies) and added to the cells of the supernatant. Cells were washed once with PBS, resuspended in 200 µL of binding buffer (Cat. no. 556454, BD Biosciences) and stained with 5 µL of Annexin V FITC and 5 µL of PI. Following a 15 minute incubation, cells were washed and resuspended in binding buffer before being analyzed with BD Biosciences FACSCalibur DxP8. The instrument was equipped with three lasers with excitation wavelengths of 407, 488, and 637 nm and eight detectors for fluorescence. To determine number of live, apoptotic and necrotic cells, data were analyzed with FlowJo vX.0.7.

4.2.7 Mitochondrial Membrane Potential Assay

The effect of CAP on cancer cells was visualized with Mitotracker Red CMXRos (Cat. no. M7512, Life Technologies) a mitochondrial-specific, non-cytotoxic dye that accumulates in the cell's mitochondria in a membrane potential-dependent manner. Briefly, 25,000 cells per well were seeded in 24-well plates and cultured overnight. Cell culture media was replaced with 600 µL of fresh media to remove any of the unbound cells. The adherent cells were treated with plasma for 60 seconds and incubated for an additional 6, 12 and 24 hours before staining. After incubation with MitoTracker Red, cells were fixed in 4% paraformaldehyde and permeabilized with 0.5% Triton X in blocking buffer (50% (w/v) BSA in PBS). They were subsequently stained with Alexa Fluor 488 Phalloidin (Cat. no. A12379, Life Technologies) for visualizing F-actin followed by 4', 6-diamidino-2-

phenylindole (DAPI) (Cat. no. 62247, ThermoFisher) for identifying the cell nucleus. Confocal imaging was performed with an Olympus IX81 laser-scanning microscope (Olympus, Tokyo, Japan) for visualizing the cell mitochondria. A decrease in red pixel intensity signifies a decrease in mitochondrial membrane potential.

4.2.8 Nascent Protein Synthesis Assay

Cells were prepared as described in section G, before undergoing 60 seconds of plasma treatment and further incubation for 6, 12 and 24 hours before staining. Nascent protein synthesis was determined using Click-iT Plus O-propargyl-puromycin (OPP) Alexa Fluor 488 protein synthesis assay kit according to the manufacturer's instructions (Cat. no. C10456, Life Technologies). Briefly, cells were incubated with 20 μM Click-iT OPP working solution for 30 min, fixed with 4% paraformaldehyde in 1X PBS and permeabilized with 0.5% Triton X. Cells were then incubated with Click-iT Plus OPP reaction cocktail for 30 min at room temperature protected from light, followed by incubation with Alexa Fluor 594 Phalloidin (Cat. no. A12381, Life Technologies) and DAPI (Cat. no. 62247, ThermoFisher), a blue stain to label nuclei. Nascent protein synthesis was assessed with confocal microscopy (Olympus IX81) by determining signal intensity in the green fluorescence channel. Loss of green pixel intensity, indicative of OPP expression, signifies a decrease in the rate of protein synthesis.

4.2.9 Image and Statistical Analysis

All experimental results were obtained from three independent experiments performed in triplicate with the exception of the MitoTracker Red assay and the Click-iT

Plus OPP protein synthesis assay, which were performed in duplicate. A total of 50 cells from 2 frames (25 cells each) were utilized for determining the pixel intensity of each stain. Results are expressed as the mean ± SD. Adobe Photoshop was used to manage the images collected for protein synthesis and MitoTracker studies. Pixel intensities were determined with ImageJ (National Institute of Health, MD, USA). Data plots and statistical analyses were performed with Prism 6 (GraphPad software, San Diego, CA, USA). The differences between groups were determined by two-tailed unpaired t-tests and data were considered significant for (*) $p < 0.05$, (**) $p < 0.01$, (***) $p < 0.001$ and (****) $p < 0.0001$. When standard deviations between groups were not equal, significance was determined using Welch corrected unpaired t-tests. Histograms were generated using mean and standard error of the mean (SEM) values. In figures 1-6, statistical significance was determined against untreated condition unless otherwise indicated.

4.3 Results

4.3.1 Real Time Monitoring of Cell Response: Treatment Duration and Discharge Voltage

Figure 4.1 and 4.2 show the effect of plasma treatment duration and discharge voltage on cancer cell viability utilizing the RealTime-Glo MT Cell Viability Assay. This assay enabled continuous monitoring of cell response via repeated reading of the testing conditions over the course of 48 hours. The RealTime-Glo assay involved the addition of a proprietary luciferase and a pro-substrate to the culture medium prior to CAP exposure. Live cells unaffected by CAP treatment facilitated conversion of pro-substrate into a new substrate, which then diffused into the culture media. The newly generated substrate was

consumed by luciferase to produce a luminescent signal. The signal correlated with the number of viable cells after treatment since dead cells were unable to reduce the pro-substrate and therefore did not produce a signal. Percent live cells were determined with respect to the untreated control condition. More specifically, percent live cells were calculated by dividing luminescent readings of the CAP treated conditions with those of the untreated control and multiplying by 100%. Therefore, the cell viability of the untreated control was assumed as 100% and is indicated by the dotted line in Figure 4.1 and 4.2.

The viability of breast cancer (Figure 4.1 (a)) and glioblastoma (Figure 4.1 (b)) cells was quantified for up to 48 hours following CAP exposures of 30, 60, 90 and 180 seconds at 3.16 kV. A greater than 50% reduction in cell viability was recorded immediately (0 min) after treatment in both cell lines for most CAP exposure times with the exception of 180-s treatment in breast cancer cells. Indeed, data showed that 30 – 90-s CAP treatments lead to more significant reductions in viability than 180-s CAP exposure. This unexpected outcome may result from CAP generated reactive species needing time to fully become incorporated in cell culture media and come in contact with cancer cells. In fact, according to the data it is not until 20 minutes after treatment when the differences in cell viability became correlated with treatment time duration. The decrease in cell viability observed immediately after treatment was followed by a viability increase which lasted up to 6 hours. From 6 - 48 hours, cell viability steadily decreased as a function of exposure time for most CAP conditions. The delayed effect of plasma in initiating cell death may depend on the phase of the cell cycle. A previous study on CAP and keratinocytes suggested that increased amounts of reactive oxygen species (ROS) produced by plasma might cause oxidative DNA damage and delay the cell cycle (G2/M phase arrest),

corresponding to a loss of viability. Therefore, the observed delayed effect in cell viability primarily observed between 0 - 6 hours when cell viability seems to be recovering (Figure 4.1), may be linked to the amount of ROS produced by CAP. The reduction in cell viability observed between 6-48 hours is in line with previous findings reporting that the most significant CAP effect is observed at 24 and 48 hours post plasma exposure.

Despite exhibiting a similar cell viability trend in the initial hour after treatment, glioblastoma cell response differed significantly from that of breast cancer cells between 6 and 48 hours. At 24 and 48 hours, the shortest CAP exposure of 30-s ultimately amounted to no substantial reduction of glioblastoma cell viability while viability of breast cancer cells decreased by 10-30%. Plasma treatments of 60, 90 and 180-s had a more significant effect on cell viability. These results attest to the fact that different cell lines responded differently to treatment.

According to the 24-hour data collected from the 60-s treatment condition, glioblastoma and breast cancer cell viability were reported at 95% and 85% respectively. The variation in response to treatment between the two cancer cell lines was noted for all CAP exposure times. The data provided evidence that the RealTime-Glo assay could detect the cell response to plasma treatment in real time with results varying per cell line and in a CAP-exposure time dependent manner.

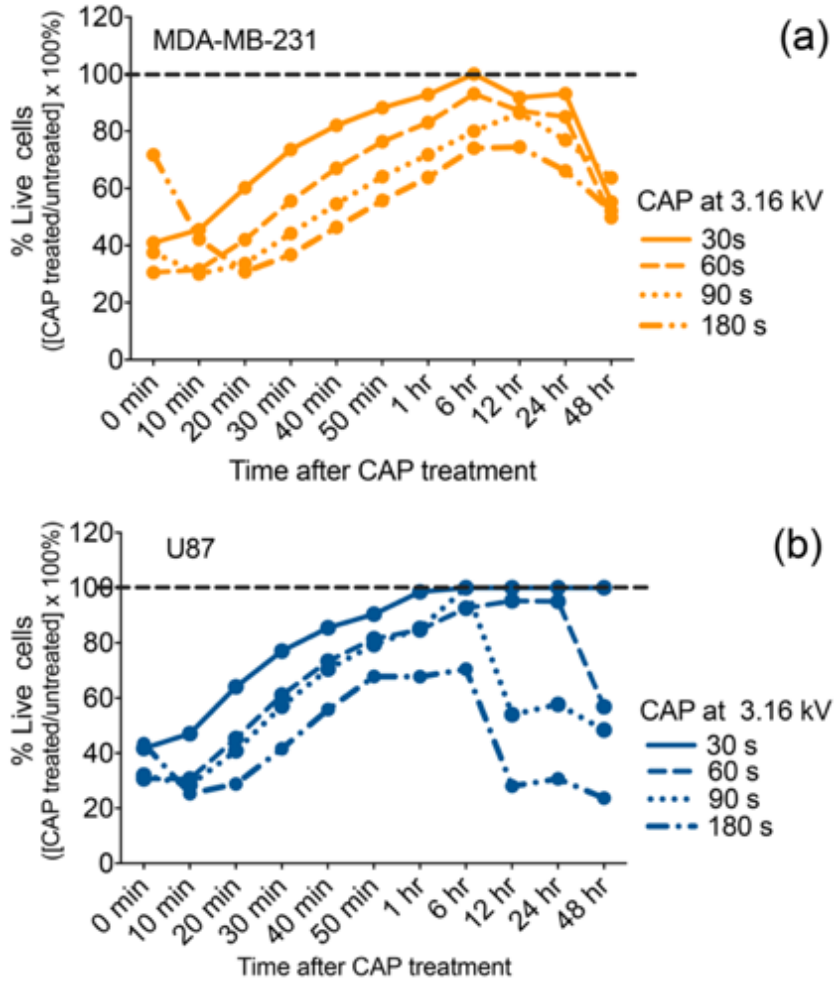

Figure 4.1 CAP treatment induces a significant reduction in cell viability over time as a function of exposure time. MDA-MB-231 breast cancer cells (a) and U87 glioblastoma (b) cells were treated with a CAP output voltage of 3.16 kV for 30, 60, 90 and 180 seconds. Immediately following treatment, RealTime-Glo MT Cell Viability Assay (Promega) was performed with a continuous read method to evaluate the response of each cell line in real time. The data were normalized to the untreated control recorded for each time point. The % cell viability of the untreated control assumed as 100% is indicated by the dotted line.

Figure **4.2** presents the same cell response pattern corresponding to the 60-s treatment in Figure 4.1. The data emphasize the variation in cell response resulting from an increase in discharge voltage from 3.16 to a 3.71 kV. Breast cancer data (Figure **4.2** (a)) revealed a statistically significant difference in cell viability between 3.16 and 3.71 kV conditions in the 6 – 48-hour time range. The earliest detectable variance in cell response observed at 6 hours post treatment, corresponded to a 50% final difference in cell viability between the two voltage conditions. In glioblastoma cells, the first significant difference in cell response was observed as early as 20 minutes after treatment.

The discharge voltage effect became more pronounced at 24 hours where a 0.55 kV increase in voltage resulted in a 70 % reduction in viability. Real time results demonstrate the important role of CAP discharge voltage in influencing cell response. Indeed, Figure **4.2** (c) reveals that a modification in voltage, translated to different cell viability outcomes not only within one cancer cell line but also between the two types of cancers investigated.

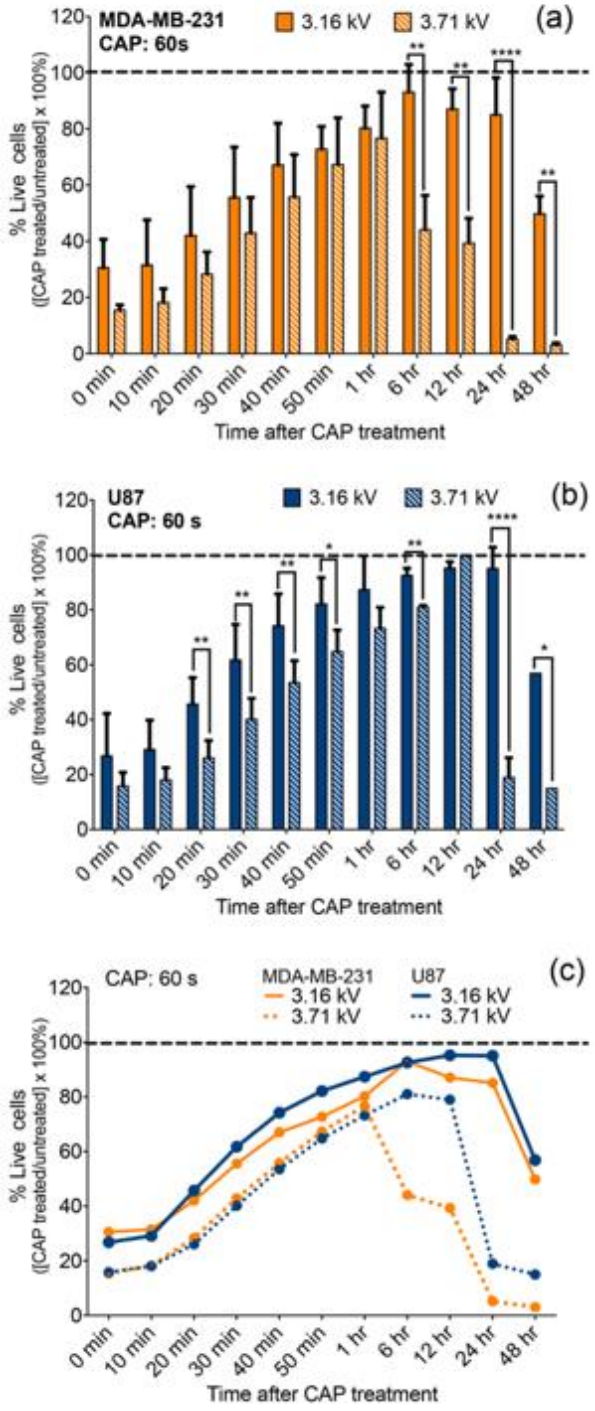

Figure 4.2 CAP effect on cell viability varies as a function of discharge voltage. Breast cancer cells (MDA-MB-231) (a) and glioblastoma cells (U87) (b) were treated with a CAP output voltage of 3.16 kV and 3.71 kV for 60 seconds. A side-by-side comparison (c)

revealed a difference in viability between the two cell lines as a function of discharge voltage. RealTime-Glo MT Cell Viability Assay (Promega) was performed with a continuous read method for evaluating cell response. The data were normalized to the untreated control condition (assumed at 100% viability) indicated by the dotted line.

4.3.2 Evaluation of H_2O_2 and NO_2^- post CAP Exposure

Figure 4.3, 4.4 and 4.5 elucidate the link between CAP discharge voltage and the concentration of reactive oxygen and nitrogen species (RONS) generated by it. The current literature in plasma medicine identifies high concentrations of CAP generated RONS as one of the primary factors linked to the effectiveness of CAP in cancer therapy. H_2O_2 and NO_2^- are two of the most-well reported and major longer-lived species produced by plasma. Hence, we monitored the levels of H_2O_2 and NO_2^- in breast cancer cells and glioblastoma cells (Figure 4.4 and 4.5).

Figure 4.3 shows the correlation between the concentration of CAP generated reactive species, exposure time and discharge voltage. The concentration of H_2O_2 and NO_2^- generated by plasma was qualified in cell culture media (no cells) for exposure times of 30 - 180 seconds at 3.16 and 3.71 kV CAP discharge voltage immediately after treatment. Figure 4.3 (a) and (b) show that the concentration of CAP generated species is well above the detection limit of 1.0 μM for H_2O_2 and 2.0 μM for NO_2^- as indicated by the dotted line. The lowest detection limit was determined by measuring the amount of H_2O_2 and NO_2^- in untreated cell culture media. The data show 30-180 second CAP exposures generating similar quantities of H_2O_2 and NO_2^- with concentrations of both species rising as a function of increased exposure time and discharge voltage. For instance, in Figure 4.3 (a) a 180-s plasma treatment at 3.71 kV generated substantially higher concentrations of H_2O_2 than a

30-s treatment at 3.16 kV. The same observation was noted for the quantity of CAP generated NO_2^-. Altogether the data demonstrated the important role of operational parameters in influencing the amount of reactive species generated by CAP.

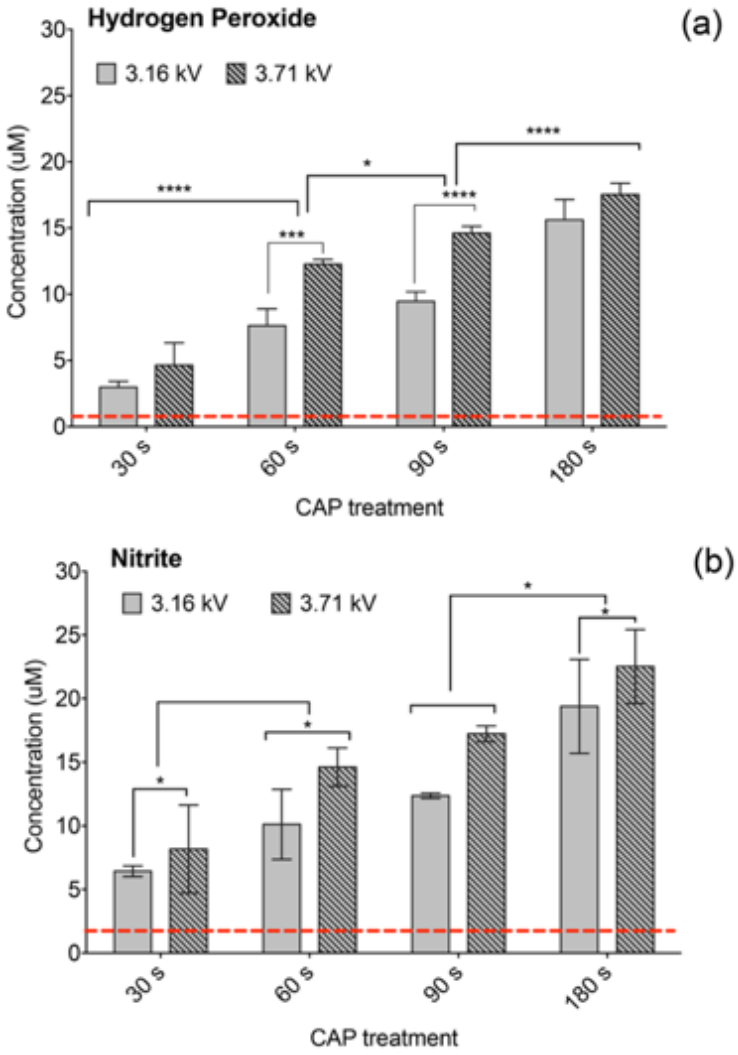

Figure 4.3 Levels of H_2O_2 and NO_2^- in cell culture media (no cells) immediately after CAP exposure. Concentration of CAP generated H_2O_2 (a) and NO_2^- (b) was measured in cell culture media for CAP exposures of 30, 60, 90, 180 seconds with 3.16 or 3.71 kV. Levels of CAP generated H_2O_2 and NO_2^- rise with increasing discharge voltage and

exposure time. The lowest detection limit indicated by the dotted line is the amount of H_2O_2 and NO_2^- in untreated cell culture media.

Figure 4.4 and 4.5 highlight the levels of exogenous and endogenous H_2O_2 and NO_2^- within each cell culture. Given that at high delivery power, plasma produces higher levels of H_2O_2 and NO_2^-, we investigated the changes in quantities of H_2O_2 and NO_2^- over the course of 48 hours in the presence of cancer cells. Cell behavior was evaluated by comparing CAP treated conditions with controls. The selected control conditions included: 1) untreated cells and 2) CAP treated media. The amount of H_2O_2 and NO_2^- in untreated cells (Control 1) was reported to be at less than 0.5 μM for all post treatment time points ranging from 0-48 hours. The amount of H_2O_2 and NO_2^- in CAP treated media (Control 2) decayed over time as these species are highly unstable in aqueous solution.

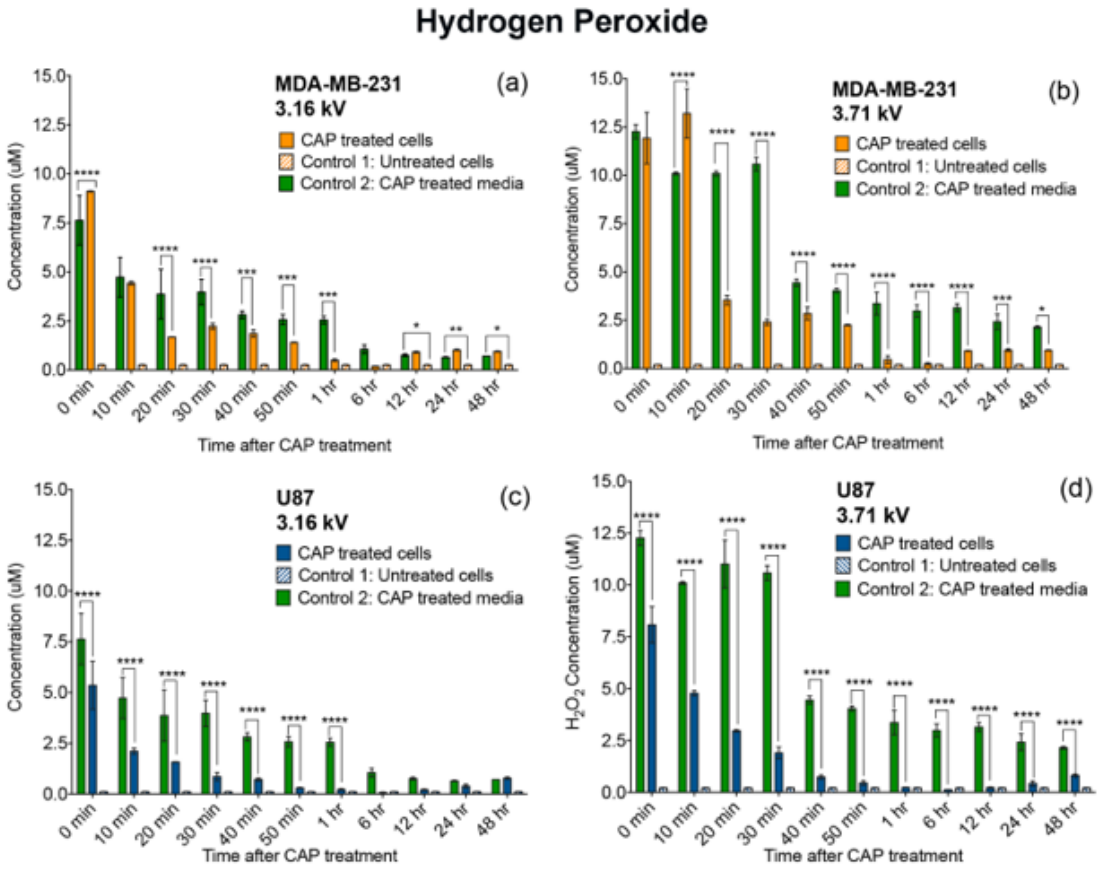

Figure 4.4 CAP generated H_2O_2 becomes metabolically degraded by cancer cells. Cells were treated with a CAP output voltage of 3.16 kV or 3.71 kV for 60-s and the effect of H_2O_2 was observed over the course of 48 hours. CAP treated MDA-MB-231 breast cancer cells (a-b) and U87 glioblastoma cells (c-d) metabolically degraded H_2O_2 starting immediately after CAP exposure. Levels measured in the CAP treated cells were compared with those of Control 1 (untreated cells) and 2 (CAP treated media).

We showed that the rate of H_2O_2 consumption varied per cell line as a function of CAP discharge voltage (Figure 4.4). A comparison over time of the CAP treated cells with CAP treated media control revealed that cancer cells metabolically degrade the generated H_2O_2. The rate of H_2O_2 consumption varied as a function of CAP discharge voltage. An

increase in plasma discharge voltage from 3.16 to 3.71 kV was accompanied with an increase in the rate of H_2O_2 metabolic degradation between 0-40 min after treatment.

In a similar trend, the rate of CAP generated NO_2^- consumption varied over time as a function of discharge voltage (Figure 4.5). Significantly higher levels of NO_2^- were detected at 24 and 48 hours of treatment compared to the CAP treated media (control 2). These results reveal that CAP not only delivers NO_2^- to cells but may also trigger NO_2^- production. Therefore, it seems likely that the demonstrated success of CAP generated RONS is due to the fact that cells consume plasma generated RONS while also perhaps secreting small amounts of RONS in cell culture media as indicated by a previous study. While the role of extracellular H_2O_2 and NO_2^- in the effectiveness of CAP therapy remains to be further evaluated, altogether the data revealed the cellular response to CAP exposure in terms of H_2O_2 and NO_2^- uptake or release, varies not only per cell line but also due to adjustments in CAP discharge voltage.

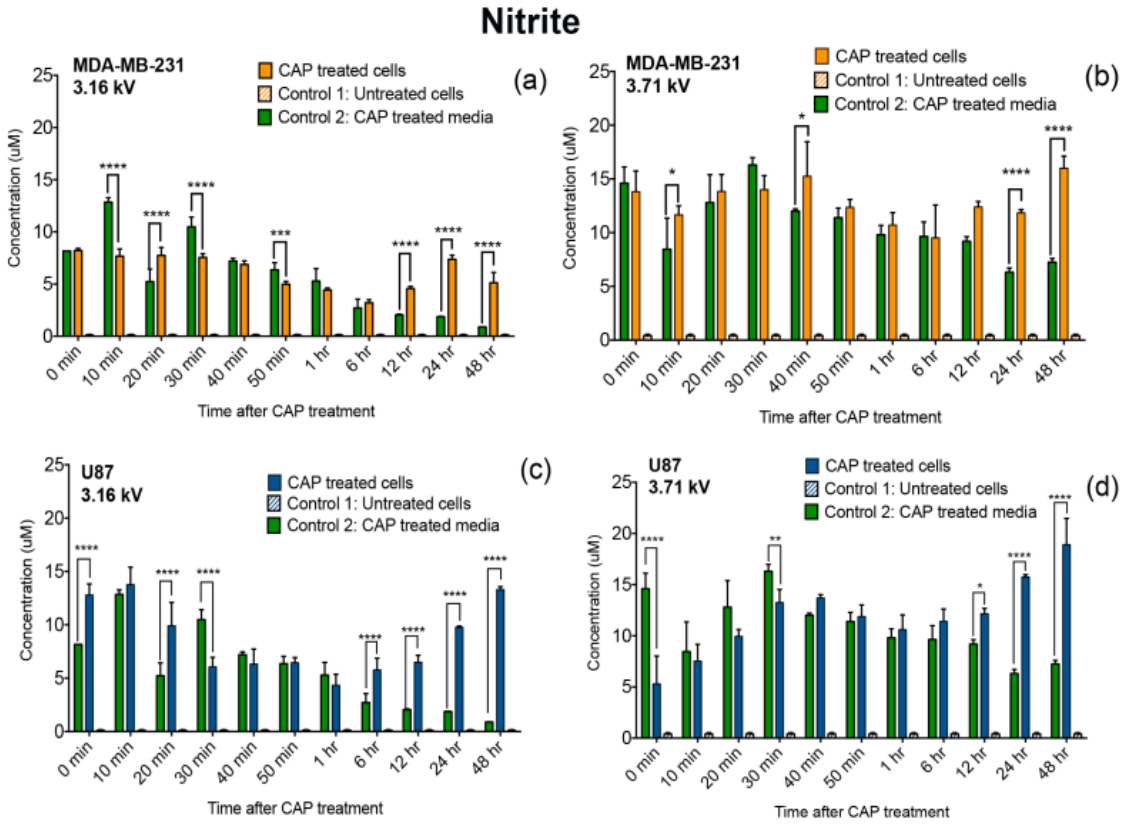

Figure 4.5 Accumulation of NO_2^- in cancer cells. MDA-MB-231 breast cancer cells (a-b) and U87 glioblastoma cells (c-d) were treated with a CAP output voltage of 3.16 kV or 3.71 kV for 60-s and were monitored over the course of 48 hours. Accumulation of NO_2^- in cancer cells post CAP exposure was estimated with by Griess reagent assay. NO_2^- levels in CAP treated cells were measured and compared with those of untreated cells (Control 1) and plasma treated media (Control 2).

4.3.3 CAP Induced Apoptosis

The results of 24-hour plasma treatment has been extensively investigated, while there is very little data on the immediate apoptotic effect of CAP. Here we determine the overall apoptotic effect of CAP over the course of 48 hours starting immediately after

treatment. The testing was conducted in 24-well plates and therefore the data are not directly comparable to the data in Figure 4.1 - 4.5 collected in 96-well plates. CAP induced apoptosis was expected to decrease due to the 24-well plates' larger volume and cell number per well. Nevertheless, the effect of CAP in inducing apoptosis is still evident in Figure 4.6.

Apoptosis was investigated by flow cytometric analysis in breast cancer and glioblastoma cells stained with Annexin V and propidium iodide. Exposure of cells to CAP (3.16 kV) for 60-s resulted in an accumulation of apoptotic cells where apoptosis was induced in a slow time-dependent manner as indicated in Figure 4.6 (a) and (b). CAP treated cancer cells showed a higher apoptotic activity than untreated control for the majority of the post treatment time points. Furthermore, the trend in the rate of apoptosis varied per cell line in the first hour after CAP exposure. For instance, immediately (0 min) upon treatment, glioblastoma cells revealed a 70% increase in the rate of apoptosis in contrast to breast cancer cells. Overall the results in Figure 4.6 attest to the varying effect of CAP on different cancer cells.

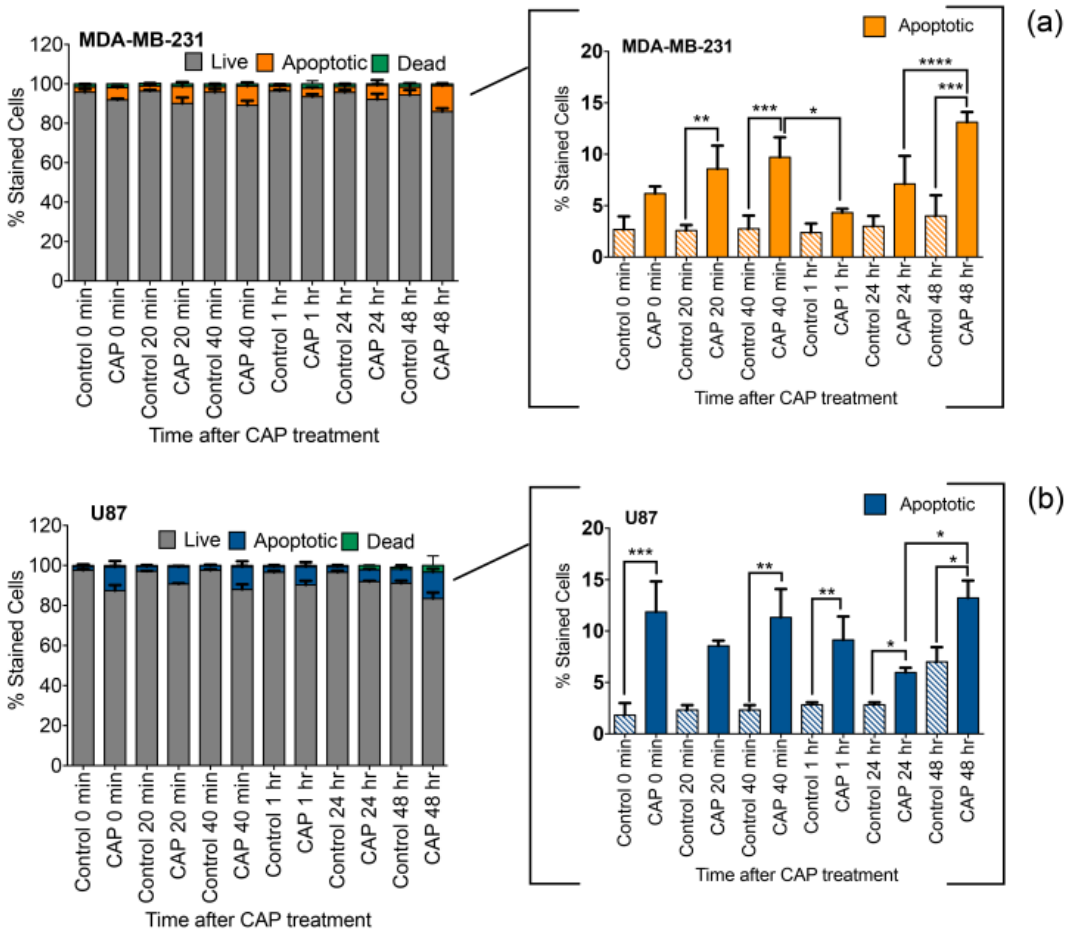

Figure 4.6 CAP exposure and apoptotic cell death. Annexin V assay of MD-MB-231 breast cancer cells (a) and U87 glioblastoma cells (b) treated with 60-s CAP at 3.16 kV. Apoptosis is presented as the percent stained fraction post treatment with respect to the untreated control.

4.3.4 CAP-Induced Mitochondrial Dysfunction

Mitochondria produce ATP, the primary energy source used in cells, via the citric acid cycle and oxidative phosphorylation. Their primary role of cellular energy production makes them a major source of cellular ROS (including H_2O_2) and oxidative stress which, if excessive, will initiate the collapse of the mitochondrial transmembrane potential and

apoptosis [102]. Here we use the MitoTracker Red CMXRos dye to investigate possible involvement of the mitochondria in the pathways leading to apoptosis. CMXRos is a non-cytotoxic dye that accumulates in mitochondria in a membrane potential-dependent manner; when mitochondrial membrane potential is reduced, less dye enters mitochondria. Data are presented in Figure 4.7. While no significant differences in membrane potential are observed between 0-60 minutes post CAP exposure (data not shown), mitochondrial membrane potential decreases by 6 hours and remains decreased at 24 hours post treatment. Data show a 20-50% decrease in pixel intensity at 6 - 24 hours post treatment compared to the untreated condition for both cell lines. In Figure 4.7 (b) and (f) cells exhibit a decrease in red pixel intensity indicative of loss in mitochondrial membrane potential. Unlike the cell viability and ROS studies, this investigation was conducted in 24-well plates instead of 96-well plates. The plasma effect is expected to reduce when the volume of cell culture media and cell number are increased but treatment parameters such as discharge voltage and CAP exposure time remain the same. The results collected are not directly comparable with those of sections 4.3.1 - 4.3.3 however they reflect the overall impact of CAP in activating cell signaling pertaining to apoptosis.

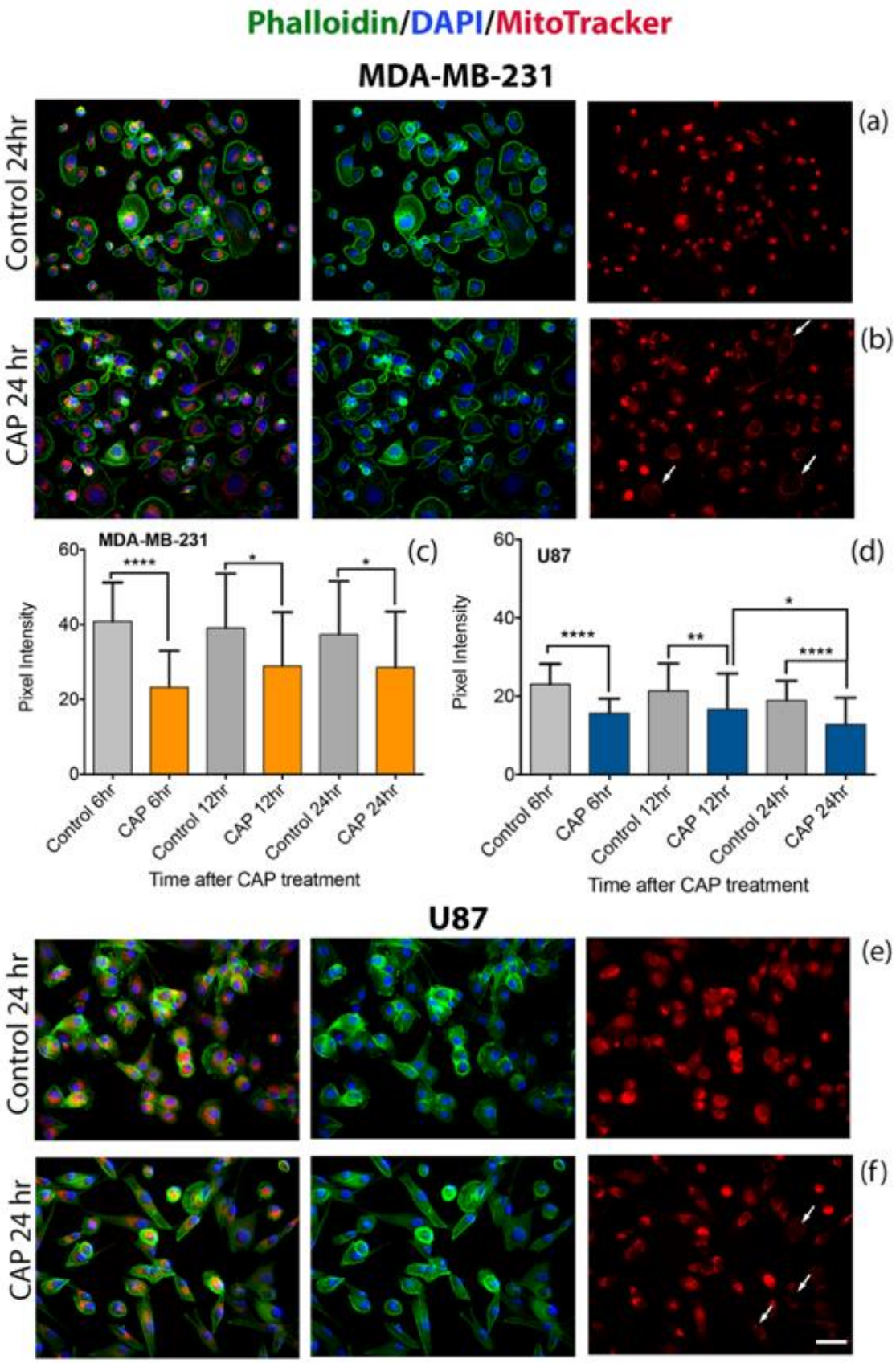
Phalloidin/DAPI/MitoTracker
MDA-MB-231
Control 24hr
CAP 24 hr
(a)
(b)
MDA-MB-231
(c)
Pixel Intensity
60
40
20
0
****
*
*
Control 6hr
CAP 6hr
Control 12hr
CAP 12hr
Control 24hr
CAP 24hr
Time after CAP treatment
U87
(d)
Pixel Intensity
60
40
20
0
****
**
*
****
Control 6hr
CAP 6hr
Control 12hr
CAP 12hr
Control 24hr
CAP 24hr
Time after CAP treatment
U87
Control 24 hr
CAP 24 hr
(e)
(f)

Figure 4.7 CAP exposure reduces mitochondrial membrane potential in cancer cells. Immunofluorescence staining of Actin (phalloidin) green, nucleus (DAPI) blue and MitoTracker Red of breast cancer MDA-MB-231 cells (a, b) and glioblastoma U87 cells (e, f) at 24 hours. Subcellular distribution of MitoTracker Red was revealed by confocal microscopy. The white arrows in (b) and (f) point to cells exhibiting a decrease in red pixel intensity indicative of a loss in mitochondrial membrane potential due to CAP exposure. Pixel intensity values of 50 cells (two frames per experiment) reveal the distribution of mitochondrial membrane potentials at 6, 12 and 24 hours post CAP exposure (c, d); Scale bar (bottom image): 10 μm.

4.3.5 CAP in Protein Synthesis

The overall rate of protein synthesis within cells is highly regulated to meet the needs of cells and tissues; it is reduced when nutrients are limited and when cells die and is increased when cells respond to stress [103]. The impact of CAP on the rate of protein synthesis in cancer cells, was assessed with a Click-iT Plus OPP assay by incorporating (OPP) as a proxy for total protein synthesis (Figure 4.8). O-propargyl-puromycin (OPP) is able to tag newly synthesized peptide chains and thus to visualize the proteins being made within the time of incubation. OPP fluorescence signal was compared between different post exposure time points and the untreated control (no CAP) condition. CAP treatment results in a decrease in OPP fluorescence (green) compared to untreated controls. Similar to the mitochondrial membrane potential study, the testing was conducted in 24-well plates which allowed for a larger cell number and volume of cell culture media. While the plasma effect may be reduced in comparison to treatment in 96-well plates, the impact of CAP on

the rate of protein synthesis is indisputable. OPP fluorescence decreased significantly between 12 and 24 hours in breast cancer cells (Figure 4.8 (c)), and between 6 and 24 hours in glioblastoma cells (Figure 4.8 (e)), indicative of a reduction in the rate of protein synthesis. Figure 4.8 (a-b) and (d-e) display a decrease in OPP fluorescence at 24 hours post CAP exposure compared to untreated condition for both cell lines. These findings are indicated with white arrows in Figure 4.8 (b) and (e), which point to cells that have lost green pixel intensity indicating a reduction in protein synthesis.

The literature reveals that a reduction of protein synthesis activity indicates ongoing stress in cells and/or apoptosis [103]. Therefore, the decrease in OPP fluorescence seen at 24 hours post CAP exposure may be linked to the CAP induced apoptosis.

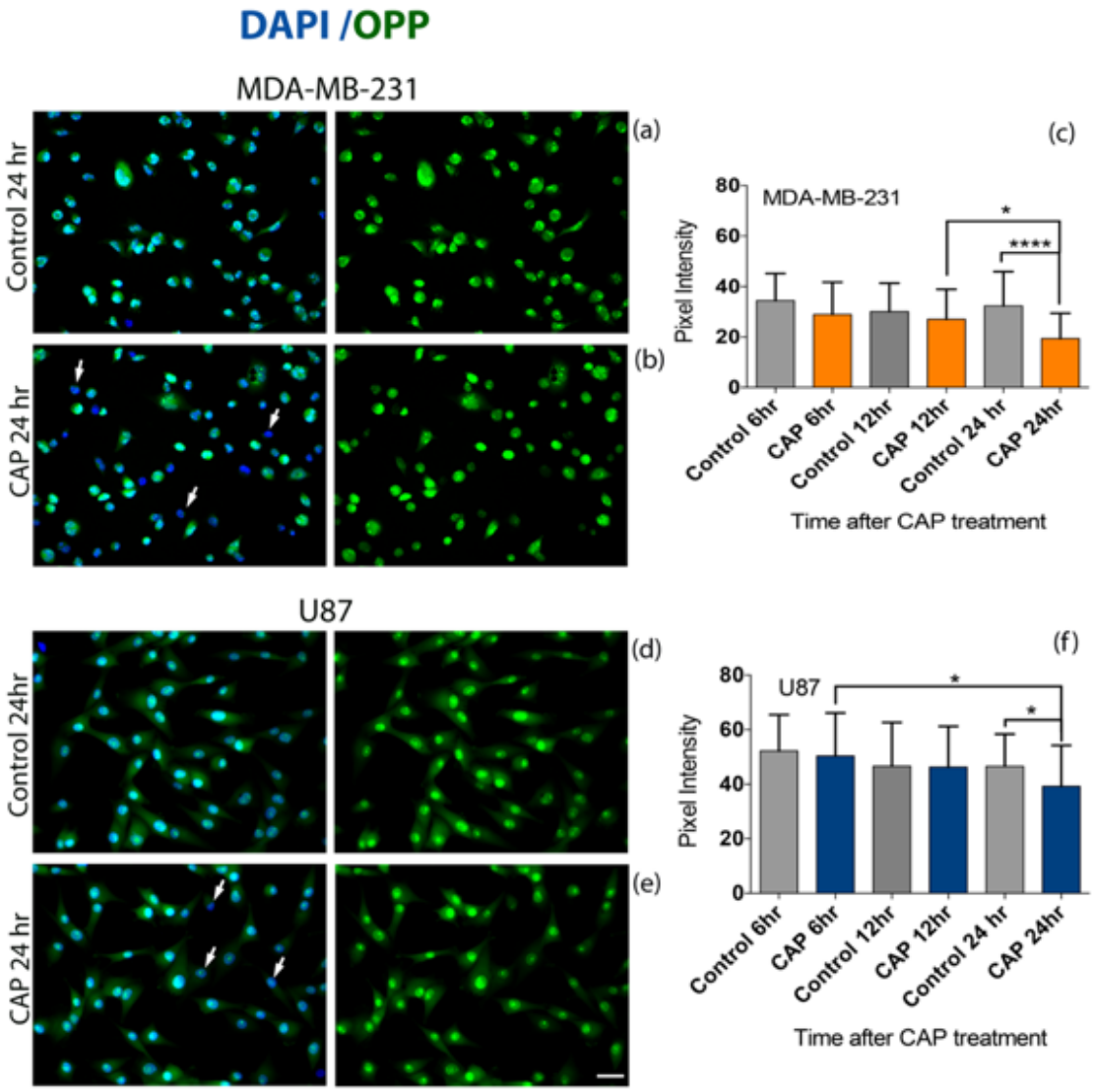

Figure 4.8 CAP exposure reduces protein synthesis in cancer cells. Cells were treated with 3.16 kV CAP for 60-s and compared to the untreated (no CAP) control condition. The Click-iT Plus OPP Alexa Fluor 647 Protein Synthesis Assay Kit was used to measure protein synthesis. Fluorescence intensity of 50 MDA-MB-231 breast cancer cells (a, b) and 50 U87 glioblastoma cells (d, e) from two experiments were quantified. Subcellular distribution of Click-iT Plus OPP staining (green) was revealed by confocal microscopy. Expression of OPP decreased between 12 and 24 hrs in MDA-MB-231 cells (c) and

between 6 and 24 hrs in U87 cells (f). A decrease in pixel intensity correlates with a decrease in the level of protein synthesis. White arrows in (b) and (e) indicate the loss of OPP (green) in cells. The cell nucleus is visualized with DAPI in blue. Scale bar (bottom image): 10 μm

4.4 Discussion

In this study, we have demonstrated that instantaneous CAP response can be effectively monitored by RealTime-Glo Assay with results interpreted as cell viability (Figure 4.1). CAP reduced cell viability as a function of discharge voltage and treatment time. The most significant reduction in cell viability was noted under the highest discharge voltage and exposure time (Figure 4.1 and 4.2). This observation is consistent with previous findings suggesting that longer CAP exposures result in cancer cells becoming increasingly less resistant to treatment. Therefore, the effectiveness of CAP therapy can be improved by adjusting discharge voltage or exposure time, which in turn control the amount of CAP generated RONS.

Based on previous studies, the ROS and RNS produced by plasma are essential in generating positive treatment outcomes by reducing cell viability and initiating apoptosis [104]. Indeed, the chemical similarities between species created in plasma and those known to be involved with actions of the innate immune system suggest that CAP-generated RONS are the primary reason for the success of this therapy in treating cancers [105]. In Figure 4.3, the quantity of the H_2O_2 and NO_2^- generated by CAP was dependent on CAP exposure time and discharge voltage. Furthermore, the incremental adjustments in discharge voltage significantly impacted cell behavior in the context of RONS

consumption by cancer cells (Figure 4.4 and 4.5). This suggests that if plasma were to be operated at different delivery power and exposure times, the variations in the amount of RONS generated would be significant (Figure 4) and therefore the effect on the different types of cancer cells may vary (Figure 4.1 and 4.2). Studies have also shown that low plasma concentrations are responsible for inducing mutagenesis and cell proliferation in tumor cells. Kalghatgi showed that a low plasma concentration enhances endothelial cell proliferation due to CAP generated ROS which mediated FGF-2 release [106] . High ROS levels not only inhibit cell proliferation, but also induce a high cytotoxic effect to the cell and can lead to apoptosis of a wide range of tumors. Therefore ROS is described as potentially harmful to cellular metabolism since it impacts cell function by altering cell development, growth, survival and tumorigenesis [107].

The observed decrease in H_2O_2 concentration over time (Figure 4.5) was in line with recent data suggesting that cancer cells have the ability to quench ROS more effectively [90,108,109]. Different biochemical changes including: generation of reactive oxygen species (ROS), calcium flux, caspase activation, loss of mitochondrial membrane potential and deregulation in protein synthesis have been reported as essential events that commit cells to undergo apoptosis [102]. CAP decreased cell viability and induced apoptosis as measured by a loss of mitochondrial potential and deregulation of OPP expression – indicative of the rate of protein synthesis (Figure 4.7 and 4.8). The investigated cancer cell lines revealed a statistically significant reduction in mitochondrial membrane potential at 6, 12 and 24 hours after treatment (Figure 4.7) associating the inability to retain mitochondrial membrane integrity to CAP exposure. The mitochondria-mediated signaling pathway that is responsible for initiating apoptosis is associated with

the release of cytochrome c from mitochondria into the cytoplasm. Cytochrome c is able to then bind to the adaptor molecule apoptotic protease activating factor-1 (Apaf-1) and subsequently activate caspase-9 responsible for the initiating apoptosis [110]. A previous study attested to the significant role of ROS in the mitochondrial apoptotic pathway by showing that the accumulation of ROS in the mitochondria was able to enhance apoptosis via reduction of mitochondrial potential, initiation of mitochondrial oxidation stress, and releasing cytochrome c into the cytosol [111].

Following CAP treatment, we also observed a general predisposition toward a reduction in the levels of protein synthesis. This suggested that CAP therapy may influence regulation of protein synthesis, which in turn impacts cancer development and growth.

The results presented elucidate how discharge voltage and treatment duration play a role in modifying plasma composition. The findings offer potential opportunities for developing an adaptive plasma system as shown in Figure 4.9. The new platform is intended for monitoring the cellular response to CAP in a continuous read method with RealTime-Glo assay serving as part of the overall feedback system. The data collected will be analyzed by a feedback algorithm which will rely on viability measurements of healthy and cancerous cells to predict the optimal amount of 1) delivery power and 2) exposure time. These two parameters will regulate the intensity of CAP and therefore the amount of RONS delivered to cells during treatment.

The feedback control algorithm, will be developed according to nonlinear model-predictive controls (MPC) [112]. MPC or receding-horizon control is a strategy used to implement numerical solutions of an open-loop optimization in the form of feedback. MPC is particularly desirable for the proposed adaptive plasma platform, as the treatment

conditions will be determined in an optimal fashion to maximize the decay rate of the tumor. The algorithm has been shown to leverage a model of plasma tumor interactions [113]. The proposed adaptive CAP system will rely on findings and methods presented in this work and, utilize theory and practice of an innovative modern control system that will advance the application of plasma in cancer treatment. The feedback system will employ adaptive properties of CAP to yield optimal and appropriate treatments tailored to real-time diagnostics, while laying a foundation for personalized adaptive cancer therapy.

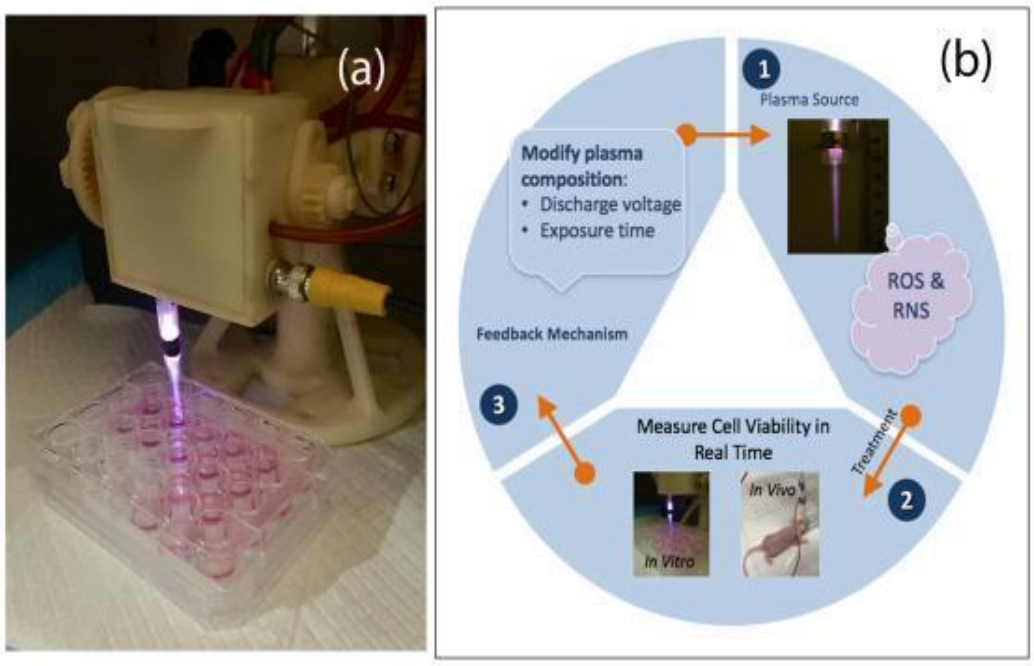

Figure 4.9 CAP device (a) and adaptive plasma platform (b). The platform monitors cellular response to CAP i*n vitro* and *in vivo* in a continuous read method. A feedback mechanism utilizes real-time data to determine the optimal amount of discharge voltage and exposure time to improve treatment outcomes and decrease cancer cell viability.

4.5 Conclusions

In summary, the findings reveal compelling evidence in support of the important roles played by the adaptive properties of CAP, treatment duration and discharge voltage, in mediating cancer suppression. Through the formation of reactive species (NO_2^-, H_2O_2 and likely others, e.g., OH, O_2, $ONOO^-$, NO) in cell culture media, we observed a reduction in cell viability dependent on CAP parameters. This ultimately led to apoptosis via changes in the mitochondrial membrane potential and the rate of protein synthesis**.** Therefore, the optimization of CAP operational parameters will be essential in providing long-lasting outcomes in anti-cancer therapy.

In addition, we outlined a potential device approach, which will rely on the presented adaptive properties of plasma for developing a feedback mechanism and optimizing plasma dosage. Following plasma exposure, it will be important to evaluate changes in cell response. The feedback mechanism will rely on real-time monitoring of cancer cell response *in vitro* and *in vivo*. We believe that the work presented here will lead to the development of a new CAP platform. This will serve as the foundation to propel CAP therapy to the forefront of other well-established therapies associated with cancer treatment. Moreover, the findings of this study will serve as a template for plasma medicine researchers to develop more robust and efficient devices that offer selective annihilation of cancer cells, while leaving healthy cells unharmed.

Chapter 5

Cold Atmospheric Plasma Enhances Sensitivity to Temozolomide in Glioblastoma U87MG Cells

ABSTRACT

Despite temozolomide (TMZ) being widely accepted as a key chemotherapeutic agent that can prolong glioblastoma patient survival, treatment failures and recurrence cases are still observed. We investigate whether Cold Atmospheric Plasma (CAP) can enhance TMZ cytotoxicity on U87MG cells. Cell responses to a single CAP treatment followed by repeated TMZ treatments was monitored with a cell viability assay. The results showed that TMZ combined with CAP inhibits cell viability of U87MG cells by a larger measure than treatment with only TMZ. CAP treatment also decreased cell migration, inhibited α6 and αv integrin expression and enhanced G2/M arrest. The results suggest that CAP could be considered as a combined treatment method against glioblastoma by sensitizing U87MG to TMZ.

5.1 Introduction

Glioblastoma multiforme (GBM) is the most common and lethal brain tumor with a median survival of 14-15 months. The current standard therapy includes maximum debulking surgery, radiation and treatment with the alkylating agent temozolomide (TMZ), also referred to as Temodar® [114]. The response to TMZ treatment is often associated

with O^6-methylguanine-DNA methyltransferase (MGMT) expression. MGMT is a repair enzyme that protects cells against DNA damages induced by alkylating agents such as TMZ. In patients with positive responses to TMZ treatment, the MGMT promoter gene is methylated and the enzyme is not expressed. Since the introduction of this drug, it has become clear that not all patients will benefit to the same extent. Overexpression of the MGMT gene results in resistance to TMZ. Additional cases in which MGMT is not the primary determinant of treatment outcomes also exist [115–120]. Thus, new treatment strategies to overcome TMZ resistance and non-cancer specific cytotoxicity are urgently needed. One of the strategies involves combining TMZ treatment with Cold Atmospheric Plasma (CAP).

In the last decade, scientists, engineers and physicians have been able to characterize CAP, optimize it for medical treatment and validate it *in vivo* and *in vitro* as a standalone cancer treatment modality [79,94]. A continued interest in this technology is fueled by the observation made from several studies suggesting that cancer cells are significantly more sensitive to CAP treatment than normal cells [95,101,121,122].

CAP is formed by applying a high electric current through a gas, a process which results in the production of electrons, ions, neutrals, UV light and reactive oxygen and nitrogen species (RONS). These reactive species have been presented by several studies as one of the key elements that have contributed to the positive outcomes achieved with CAP treatment [46,123,124]. Depending on the plasma source properties and device parameters, the composition and the concentrations of the produced CAP species vary and therefore, initiate different responses from the respective targeted tissue.

Interactions between the extracellular matrix (ECM) and cancer cells have been shown to play an important role in chemotherapy resistance and invasion [125]. Initial experiments of CAP with living cells in wound healing, demonstrated detachment of treated cells from the ECM and decreased cell migration linked to DNA damage, cell cycle arrest and integrin activation [126,127]. Integrins, have been suggested to play a protective role against chemotherapy in different tumors, including glioblastoma [118,125]. They have heterodimeric cell-surface receptors that directly bind to components of the ECM and mediate cell–matrix adhesion. Integrins are also composed of transmembrane glycoproteins α and β. When integrins are bound to ECM ligands, they induce a variety of intracellular signals including proliferation, survival, migration and invasion [128–130]. α6β1 and αvβ5 integrins are described as promoters of glioblastoma cell invasion and migration. In addition, they are the main integrins investigated in glioblastoma cell response to TMZ treatment [118,131–133]. The role of these integrins has never been reported in glioblastoma cell response to CAP or CAP-TMZ treatment.

In this study we introduce CAP as a treatment modality for increasing cell sensitivity to drugs. We show that U87MG glioblastoma cells become significantly more susceptible to consecutive temozolomide treatments when they undergo a single CAP treatment. In addition to examining the effect of plasma in different TMZ concentrations, we report the effect of CAP on cell migration, α6 and αv integrin expression and G2/M cell cycle arrest.

5.2 Methods

5.2.1 CAP Treatment and Device Operation Parameters

The CAP device was manufactured at the Micro-propulsion and Nanotechnology Laboratory of the George Washington University. The device was operated at a frequency of 12.5 kHz with a helium flow rate of 6 L/min. The helium plasma jet was generated via the dielectric barrier discharge[31]. The spot size of the plasma jet when in contact with liquid media had a diameter of about 10 mm. The distance between the plasma jet outlet and the surface of the cell culture medium was fixed at 2 cm. The device was operated in the discharge voltage range of 6.2 - 6.6 kV. Plasma treatment was performed in a direct method with cells treated in culture medium and the CAP effect was quantified for different post exposure time points (0 minutes – 48 hour).

5.2.2 Reagents and Cell Culture

Temozolomide was obtained from Life Sciences (ALX-420-044; Farmingdale, NY). It was resuspended at 20 mg/ml in 100% DMSO, aliquoted and stored at -20 ℃ in a concentration of 100 mM. The DMSO concertation in drug and media was maintained at 0.25% for all experiments.

The human cancer cell line, U87MG (glioblastoma) was purchased from the American Type Culture Collection (ATCC) (Manassas, VA). Glioblastoma cells were passaged in cell culture in Dulbecco's Modified Eagle Medium (DMEM) (Life Technologies) supplemented with 5% (v/v) fetal bovine serum (ThermoFisher) and 1% (v/v) Penicillin-Streptomycin (Life Technologies). Cells were harvested after three passages and were seeded in 24 well plates for performing experiments. The cell culture media utilized for all

experiments was prepared with 1% (v/v) fetal bovine serum and 1% (v/v) Penicillin-Streptomycin.

5.2.3 CAP and Temozolomide Treatment

Cells were seeded on 24-well plates at a concentration of 20,000 cells per well, and grown overnight with complete DMEM media containing 1% FBS and 1% penicillin-streptomycin for investigating cell response in the presence of TMZ and plasma. After a single plasma treatment of 60 or 180 seconds, the media was replaced with fresh media and/or TMZ according to testing conditions and cells were maintained under standard cell culture conditions at 37°C and 6% CO_2 (Day 0). The drug and media were replaced on alternate days (Day 2 and 4) and the cells were incubated for up to 6 days before ending the assay on Day 6. The cells were tested in the following conditions: 1) media, 2) plasma treatment, 3) TMZ treatment and 4) plasma and TMZ treatment.

5.2.4 Cell Viability Measurement

TMZ concentrations of 10, 25, 50, 100 and 250 μM were evaluated for up to 6 days with the drug being replaced every other day. TMZ concentrations of 10 and 50 μM were evaluated for additional studies on Day 1 and/or Day 6 for plasma treatments of 60 and 180 seconds. The cell viability experiments were preformed three times in six replicates per condition. CellTiter-Glo 2.0 Luminescent Cell Viability Assay (G9242; Promega) was utilized for quantifying the effect of the drug and plasma on cell viability. The assay determines the number of viable cells based on the quantification of ATP present, an

indicator of metabolically viable cells. The CellTiter-Glo 2.0 reagent was added to each well in equal volume to that of cell culture media. During the 10 minute incubation at room temperature, the reagent leads to cell lysis and generation of a luminescent signal proportional to the amount of ATP present, and thus indirectly measures cell number. After the 10 minute incubation was complete, 200 uL of reagent in media was transferred in triplicate in a 96 white walled plate and the luminescent signal was recorded in Tecan microplate reader.

5.2.5 Cell Migration Time-Lapse Studies

Time-lapse studies were performed on an Olympus IX81 microscope (Olympus America, Center Valley, PA) equipped with a motorized stage and a temperature and CO_2 controlled chamber. Using relief-contrast optics, images (10x) were taken every 10 minutes per well for an uninterrupted 16 hours and 40 minutes (100 images). Images were analyzed with a Metamorph image analysis software (Molecular Devices Corporations, Chicago, IL) where velocities and persistent displacement of 10 cells per well were calculated using the track cell module. A visual basic program assisted in data analysis. From each cell tracked, an average velocity, net displacement, and total displacement were calculated. Cell tracking was performed immediately following 180 seconds of plasma treatment (Day 0-1) and on Day 5-6 for a TMZ concentration of 50 μM. The experiments were carried out twice and in replicates of three per condition.

5.2.6 α6 and αν Immunofluorescent Staining

For experiments involving immunofluorescent staining, cells were plated onto 24 well plates and experiments were performed for cells on Day 1 and Day 6. The cell culture media was discarded, and cells were fixed in 4% paraformaldehyde (Thermo; 28906) in PBS for 20 min, and then rinsed in PBS. Non-specific staining of cells was blocked by incubating the cells for 30 min in blocking buffer (1% Bovine Serum Albumin (BSA), 1 % horse serum in 1X PBS) with 0.02% Triton-x 100. Cells were incubated overnight at 4°C in a 1:250 dilution in the appropriate primary antibodies (α3, α6 and αv) followed by 3X 10 minute washes with PBS the next day. Additionally, cells were incubated with blocking buffer for 30 minutes followed by 1 hour incubation in secondary antibody added in a 1:500 dilution. α6 was detected with rat derived GOH3 (Santa Cruz; SC-19622) and αv integrin was visualized using the goat derived CD51antibody (R&D Systems; AF1219). Nuclei were visualized using DAPI (Invitrogen Corp; D21490) in a 1:2000 dilution. Images were acquired at 20x magnification using a Nikon Eclipse TS2R and sum pixel intensity for each image was quantified using NIS Elements BR v5.00 software. (Melville, NY). Fluorescence staining was performed on Day 1 and 6 for cells treated with 180 seconds of plasma and 50 μM TMZ. The experiments were carried out twice and in replicates of three per condition.

5.2.7 Flow Cytometry and Cell Cycle Analysis

DNA staining was performed for U87MG cells treated with 180 seconds of plasma and TMZ concentrations of 10 and 50 μM. After 6 days in culture following the procedure described in section 4.2.2., U87MG cells were harvested and centrifuged at 1200 rpm for

5 min. They were further washed 2X with phosphate-buffered saline (PBS), fixed in ice-cold 70% ethanol and stored at 4°C for 2-4 days. Cells were then washed twice with PBS and incubated in the dark in PBS containing 20 mg/ml RNase A (Thermo; EN0531) and 50 mg/ml propidium iodide (PI) (Thermo; P3566) at 37 °C for 30 min. Flow cytometry data collection was performed on a BD Celesta Cell Analyzer at the George Washington University's Flow Cytometry Core Facility. The analyzer is equipped with three lasers providing excitation wavelengths of 488, 640 and 405 nm and twelve detectors for fluorescence. Data analysis for DNA content was performed with FCS 6 Express software(De Novo; Glendale, CA) for quantifying G1, S and G2/M- phases of the cell cycle. The results were reproduced with four sets of U87MG cells per condition.

5.2.8 Imaging and Statistical Analysis

Data plots and statistical analyses were performed with Prism 6 (GraphPad software, San Diego, CA, USA). The differences between groups were determined by ANOVA (Analysis of Variance) and data were considered significant for p values of less than 0.05. When standard deviations between groups were not equal, significance was determined using Welch corrected unpaired t-tests. Potential outlier values for all conditions were determined with an online outlier calculator from GraphPad which performs the Grubbs' test (ESD method). Adobe Photoshop was used to manage the images collected for all figures.

5.3 Results

5.3.1 CAP-Enhances TMZ Induced Cell Death

The anti-tumor effect of CAP as a standalone therapy in the treatment of glioblastoma and other cancers has been investigated *in vitro* and *in vivo* [43,123,134–138]. Positive treatment outcomes reported by several studies make CAP a good candidate to be evaluated as a new treatment strategy for enhancing sensitivity to TMZ treatment in glioblastoma. We evaluate the anti-tumor effect of CAP and TMZ in a U87MG cell line often investigated in plasma studies [43,123,139,140]. CellTiter-Glo 2.0 luminesce assay was utilized for monitoring cell response to CAP treatment. The utilized luminescence assay measures cell metabolic activity which serves as a proxy for cell viability (Sec. 5.2.4.). Preliminary experiments for establishing optimal CAP treatment duration revealed that 60 and 180 seconds of plasma treatment were appropriate for this study. To better understand the CAP-TMZ relation, we selected treatments that provided little to almost no effect on cell viability. A cell growth inhibition of about 15 percent was observed after 60 seconds of CAP treatment and a slightly higher reduction of 25 percent after 180 seconds of CAP (data not shown).

Cell viability response to repeated TMZ treatments of 10, 25, 50, 100 and 250 μM was initially evaluated to determine suitable TMZ doses for additional evaluation. The U87MG cell response to different TMZ doses was monitored over the course of 6 days with the drug treatment repeated on alternate days (Day 0, 2 and 4). Figure 5.1 (b) reveals the cell response to TMZ treatment 24 hours (Day 1) and 6 days from the application of the initial drug dose (Day 0). TMZ displayed no significant cytotoxic effect within the first 24 hours of treatment. On day 6, the impact of TMZ in cell response becomes more

pronounced with drug doses of 10 - 250 μM causing a significant dose depended inhibition in cell growth.

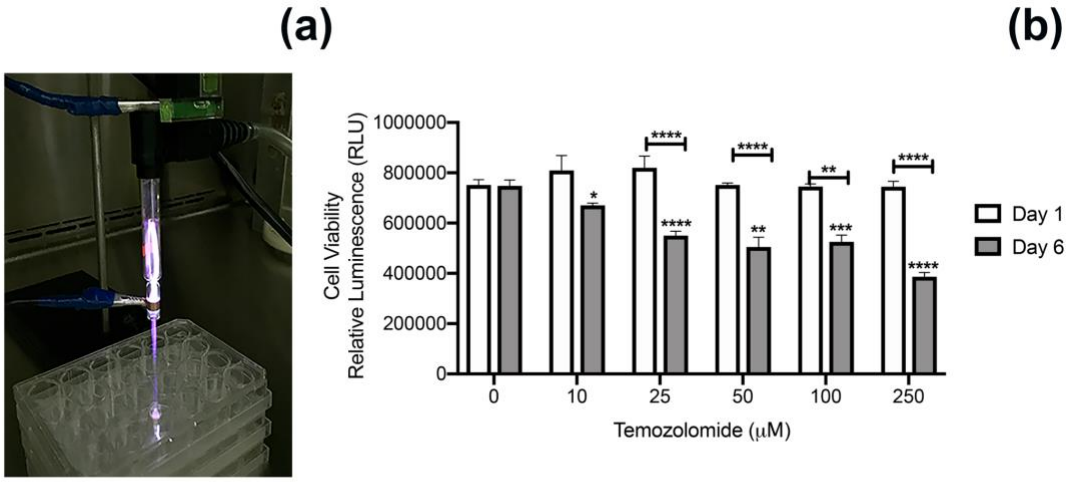

Figure 5.1 Inhibition of cell proliferation by Temozolomide. (a) The plasma device utilized for the study. (a) U87MG glioblastoma cells were treated with 10 μM, 25 μM, 50 μM, 100 μM and 250 μM of temozolomide for six days with the drug being replaced in alternate days. Cell response was recorded 24 hours and 6 days after plasma treatment. The asterisk indicates statistical significance compared to the untreated condition unless otherwise noted.

The role of 60 and 180 seconds CAP in cell sensitization was evaluated on Day 6 in the presence of a non-cytotoxic and (10 μM) and a cytotoxic (50 μM) drug dose. To better understand the effect of a combined CAP-TMZ treatment, results were compared with three control variables which included: 1) untreated, 2) CAP and 3) TMZ treated cells. The findings presented in Figure 5.2 (a) reveal that a single CAP treatment of 60 seconds did not successfully sensitize cells when combined with a non-cytotoxic drug dose nor did

it enhance the effect of a 50 μM cytotoxic dose. In contrast, the 180 seconds CAP treatment successfully sensitized cells to both TMZ doses (Figure 5.2 (b)). Results for the combined therapy of 180s CAP – 50 μM TMZ reveal a statistically significant reduction in cell viability of 15 % compared to the drug and 30 % compared to untreated. Furthermore, they emphasize the application of plasma as a standalone therapy with plasma displaying an additional 10% decrease in viability compared to combined CAP-TMZ therapy. The results also indicate that a significantly higher plasma dose is needed in order to create an irreversible effect in cell sensitization. According to the data presented, the plasma dose needs to create at least a 30% reduction in viability as a standalone therapy before it is combined with TMZ.

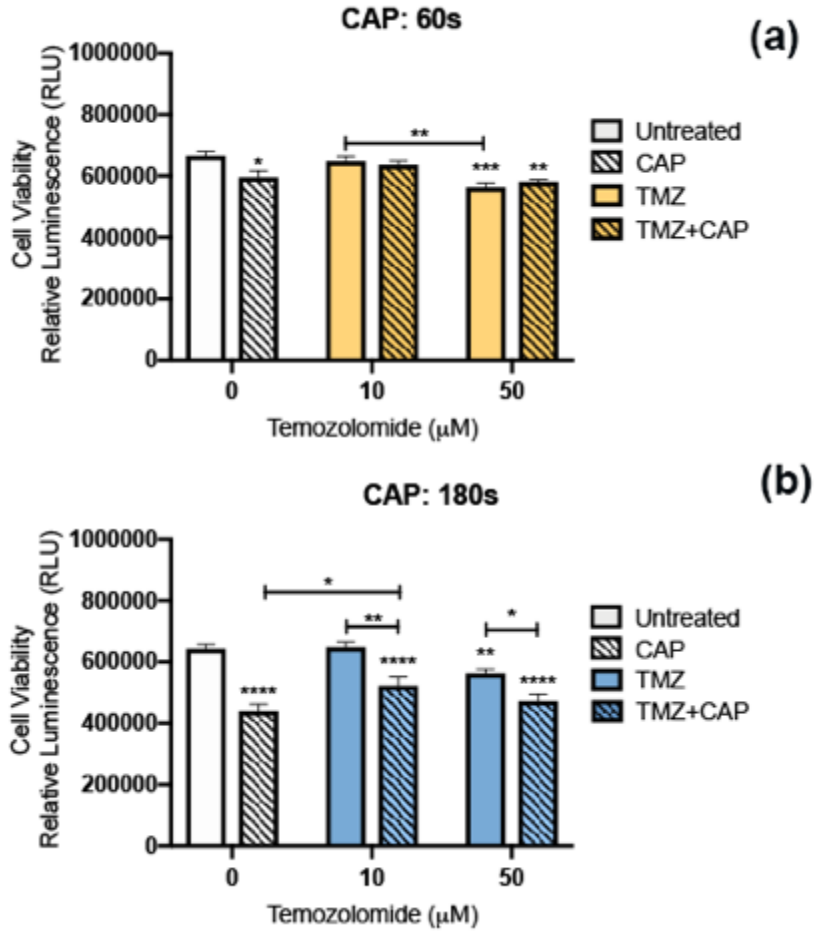

Figure 5.2 CAP sensitizes glioblastoma U87MG cells to temozolomide treatment U87MG glioblastoma cells were treated with 10 μM and 50 μM of temozolomide for six days with the drug being replaced in alternate days. Cell response six days after treatment with (a) 60 and (b) 180s of plasma, 10 and 50 μM temozolomide and plasma-temozolomide combined. The plasma treatment was performed only on once whereas the drug was replaced every two days and cell response was recorded on day 6. The asterisk indicates statistical significance compared to the untreated condition unless otherwise noted.

5.3.2 Reduced Rate of Cell Migration in CAP-TMZ Treated Cell

Using time-lapse microscopy, we next assessed the rate of cell migration of U87MG cell treated with 180 seconds of plasma (single treatment) and repeated treatments of 50 μM TMZ. The trend in cell migration was monitored for the initial 16 hours following CAP (Day 0-1) and in the last 16 hours (Day 5-6) before the treatment was completed. Representative tracks obtained from 10 U87MG cells maintained are shown in Figure 5.3 (a) and (b). The red tracks indicate the paths taken by the cells during the time in which 100 images were taken. The tracks from the CAP-TMZ treated cells are shorter than those from untreated, CAP and TMZ treated only cells (Figure 5.3) for both time point investigated. Quantification of data from 60 cells tracked for each variable are shown in Figure 5.3 (c) - (f). The effect of CAP on cell migration can be observed as early as 16 hours following CAP and TMZ treatment. Cells exposed to a combined treatment of CAP-TMZ migrated significantly slower than those exposed to only CAP or TMZ treatment. This suggests that CAP successfully enhances the anti-tumor effect of TMZ. On the last day of treatment, cells exposed to only TMZ and CAP-TMZ combined, migrate with the same velocity but have a significantly slower rate of migration than the untreated condition. Persistence, which represents the directionality of the cells motion, was also evaluated for all tested variables. Persistence was measured as the ratio between net and total displacements. Cells treated with CAP-TMZ therapy show changes in persistence compared to the control groups.

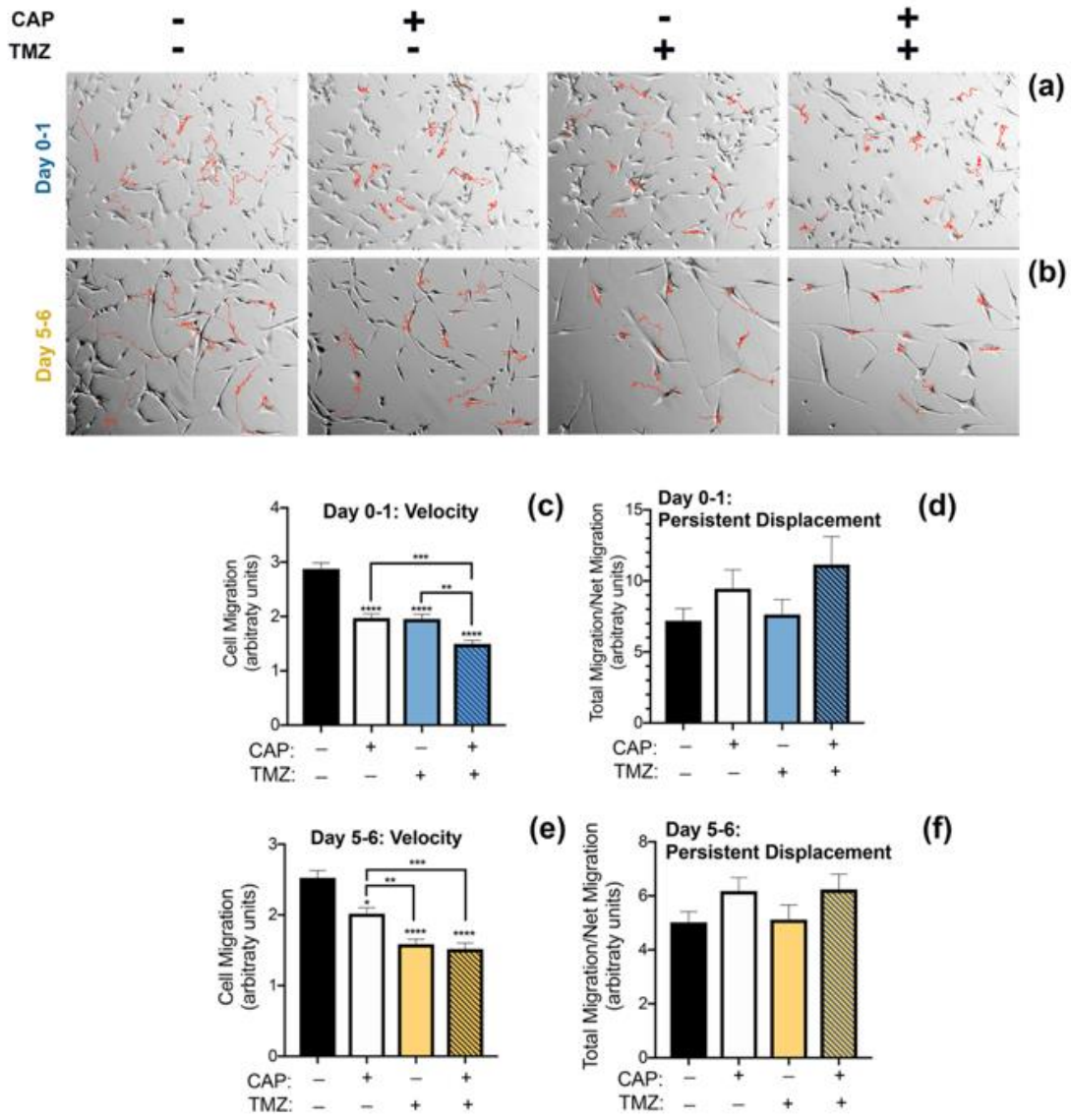

Figure 5.3 CAP reduces the rate of cell migration in U87MG cells. Time-lapse microscopy studies were performed for U87MG cell treated with 180 seconds of plasma (single treatment) and repeated treatments of 50 μM TMZ. Tracks of 10 representative cells studied over the 16 hour 40 minute time period are indicated in red for (a) Day 0 -1 and (b) Day 5- 6. The tracks traveled by cells in the CAP-TMZ condition are shorter than those for

the control variables. The graphs display calculated rate of cell velocity (c), (e) and cell displacement (d), (f) of 60 cells per each variable.

5.3.3 CAP Treatment Alters Expression of αv and α6 Integrins in TMZ Treated Cells

The expression levels of two cell surface integrins, α6 and αv, were investigated to determine if they provide indication/insight on the role of plasma in inducing/enhancing TMZ cell response. We assessed integrin expression levels in U87MG cells treated with a single plasma treatment (180 seconds) and repeated treatment of TMZ (50 μM). Fluorescence staining of cells was performed for the 24 hours and 6 day time point following plasma treatment. According to Figure **5.4** (a) and (b), CAP and TMZ do not trigger any αv and α6 integrin expression up to 24 hours after treatment. Figure 5.4 (c) and (e) show that TMZ treatment does not impact αv and α6 integrin expression on Day 6. Unlike TMZ, CAP suppresses αv and α6 integrin expression and further mediates suppression of these integrin in TMZ treated cells (Figure 5.4 (d) and (f)). These results suggest that the αv and the α6 integrin expression is a good indicator for differentiating between TMZ and CAP treatment.

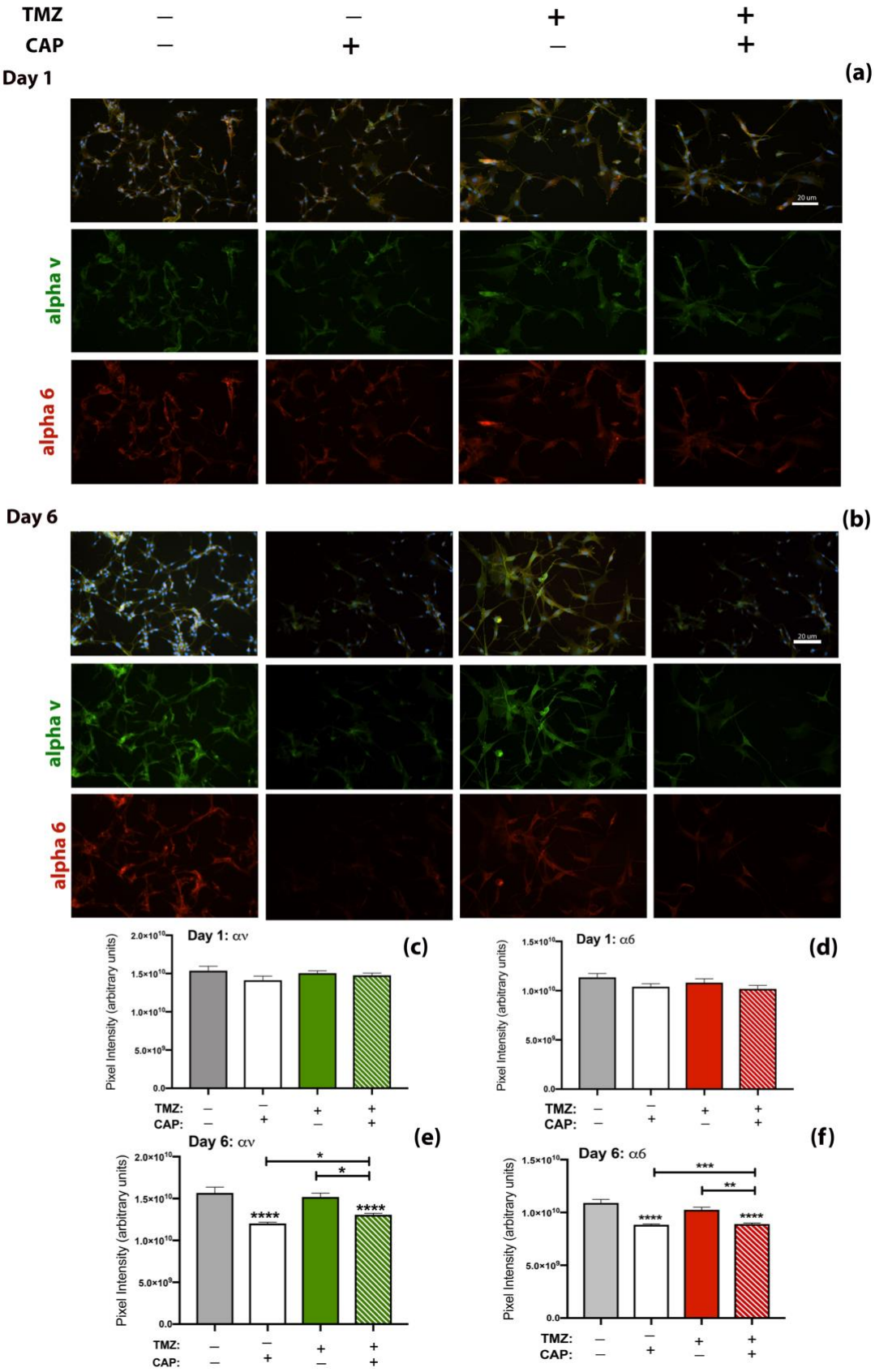
TMZ – – + +
CAP – + – +
Day 1
(a)
alpha v
alpha 6
20 um
Day 6
(b)
alpha v
alpha 6
20 um
Day 1: αv
(c)
Pixel Intensity (arbitrary units)
2.0×10^10
1.5×10^10
1.0×10^10
5.0×10^9
0.0
TMZ: – – + +
CAP: – + – +
Day 1: α6
(d)
1.5×10^10
1.0×10^10
5.0×10^9
Day 6: αv
(e)
* *
****
Day 6: α6
(f)
*** **

Figure 5.4 CAP mediated αv and α6 integrin expression in TMZ treated cells. The immunofluorescence staining was performed for U87MG cell treated with 180 seconds of plasma (single treatment) and repeated treatments of 50 μM TMZ. Representative images for each variable were taken with a 20x magnification and are shown in (a) and (b). αv integrin is shown in green, α6 integrin is shown in red and the nuclei stained with DAPI in blue. The graphs display sum pixel intensity for αv and α6 for each of the variables tested at the Day 1 and 6 timepoint (c-d). Scale bar: 20 μm

5.3.4 Cell Cycle Changes in G2/M phase

The cell cycle is an intricate sequence of events which enables cells to grow and replicate. Cells that undergo replication, move from G1 phase into the S phase for DNA synthesis. The S phase is followed by the G2 phase, where cells prepare for duplication in the M phase. In glioblastoma, DNA damage is central to the cellular response to chemotherapy and radiation and results in cell cycle arrest predominantly at the G2/M checkpoint [126,141,142]. TMZ, being a DNA alkylating agent, is also known to induce cell cycle arrest at G2/M and to eventually lead to apoptosis. To better understand how cell sensitization to TMZ occurs after CAP treatment, the cell response to CAP and TMZ was investigated in 10 and 50 μM TMZ and 180 seconds of plasma after 6 days in culture. Figure 5.5 (a) shows the DNA content measurement of all variables. G1, S and G2 peaks are indicated for each histogram. Figure 5.5 (b) presents cell distribution in each phase of the cell cycle with the data being characterized by the fraction of the cells in the G2/M– phase. The results suggest that TMZ treatment induces a delay in the progression of the U87MG cells through the cell cycle in a dose dependent manner (10 - 50 μM). This leads

to an increased number of cells at the G2/M checkpoint. Combined treatment of CAP with TMZ results in a slightly larger number of cells undergoing G2/M cell cycle arrest compared to the drug however, these results are not statistically significant as well. TMZ and CAP-TMZ combined led to a ~ 2-4 fold increase of cells in the G2/M-phase of the cell cycle compared to the CAP and untreated variable.

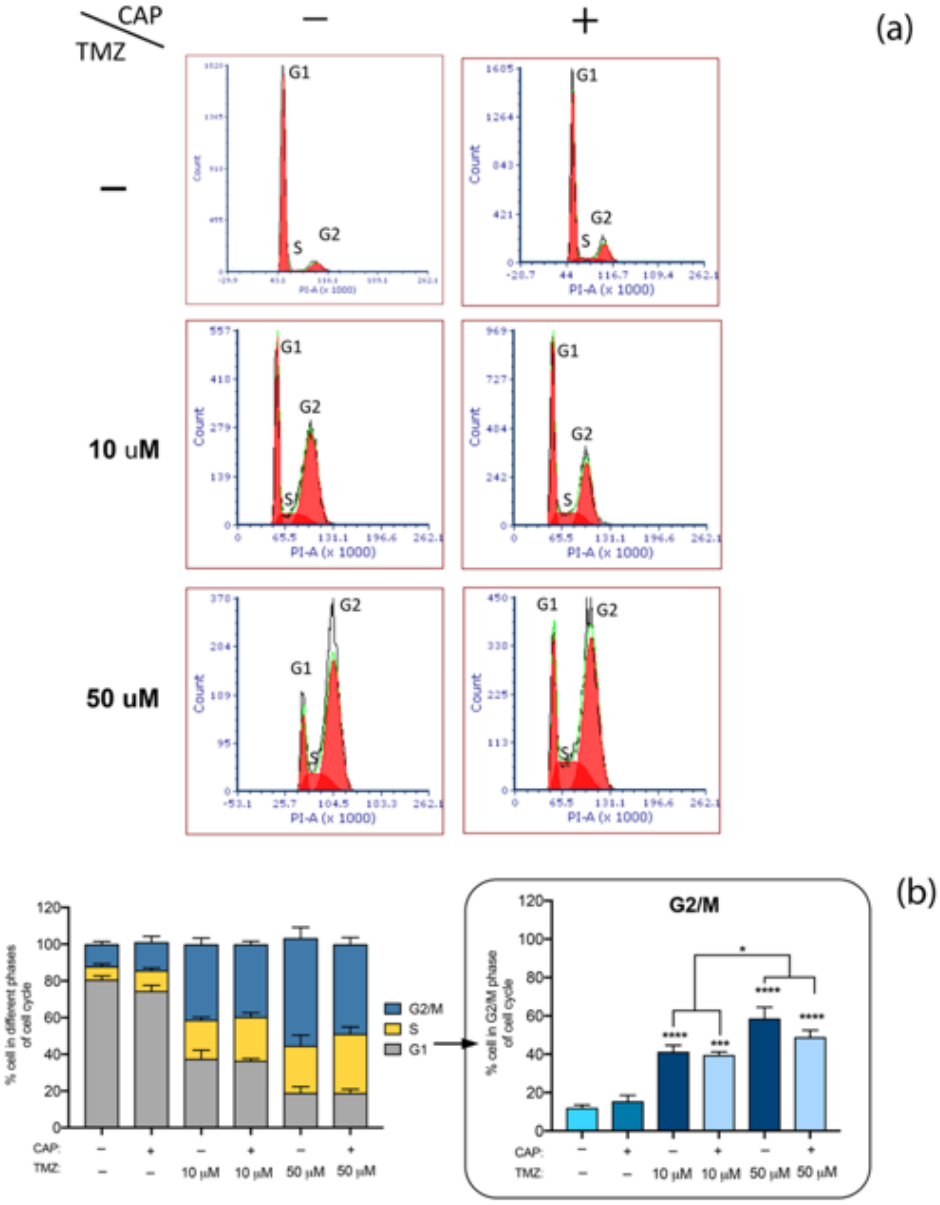

Figure 5.5 Cell cycle arrest in G2/M phase. (a) Representative histograms of U87MG cells indicating cell distribution in each phase of the cell cycle for each of the variables. (b) Cell distribution in each phase of the cell cycle with data characterized by the fraction of the cells in the G2/M–phase. Statistical significances of the observed arrest in the G2/M phase for U87MG cells six days after treatment with 180 seconds of plasma, 10 and 50 μM temozolomide and plasma-temozolomide combined. The drug was replaced in alternate days. The asterisk indicates statistical significance compared to the untreated condition unless otherwise noted.

5.4 Discussions

Resistance to TMZ in glioblastoma presents a real challenge with only ~50% of cases showing a positive response to treatment [120,143,144]. Chemotherapy resistance is a common problem, and therefore the need for technologies to overcome resistance is always on the rise [145,146]. In the present study we evaluated the role of CAP combined with TMZ and report the successful application of this technology in sensitizing cells to TMZ treatment. Note that our study is only the third one to evaluate the application of this technology in combination with drug treatment [88,147]. Substantial improvements of CAP technology over the years and positive treatment outcomes reported from *in vivo* and *in vitro* studies in glioblastoma, have made CAP an appealing treatment option for overcoming resistance to TMZ [79,94].

We investigated cell viability response to CAP treatment in the presence of 50 μM cytotoxic and 10 μM non-cytotoxic drug dose. According to previous studies, the 10 μM dose results in no significant depletion in MGMT [146] and is within the range of equivalent drug doses achieved in the cerebrospinal fluid (CSF) of patients after

treatment [148,149]. We observed that CAP could successfully sensitized cells to a non-cytotoxic drug dose (10 μM) and it further enhanced the effect of the cytotoxic dose (50 μM). The study also reveals that the success of this therapy is contingent upon the CAP dose. Specifically, CAP needs to create at least a 30% reduction in viability as a standalone therapy before it is combined with TMZ otherwise it risks being unsuccessful in the treatment of glioblastoma.

In a previous study it was reported that a CAP-TMZ combined treatment leads to a more significant cell viability inhibition than CAP alone [147]. However, our data showed a reverse pattern indicating that CAP treatment alone can create a more substantial effect on the rate of cell death compared to CAP-TMZ combined treatment. These discrepancies in treatment response can be attributed to differences in CAP devices which have presented a real challenge within the plasma research community.

The primary biological features of malignant gliomas include a high rate of tumor cell proliferation, attachment to the normal surrounding brain tissues, and a lower rate of cell migration [150]. Cell attachment mediated by cell-surface receptors known as integrins, is also crucial for cell invasion and migration [151,152]. Therefore, targeting the function of integrins such as α3, α6β1, and αvβ3 which are highly expressed in glioblastoma [128,153,154], may offer insight into the treatment of this tumor. Previous studies investigating the role of CAP in integrin expression and activation have been primarily concerned with wound healing [155–159]. Here we report for the first time on the effect that treatment with CAP-TMZ combined has on α6 and αv integrin expression and cell migration. The effect of CAP on cell migration was observed as early as 16 hours following CAP and TMZ treatment. Our results indicated that cells exposed to CAP-TMZ

combined therapy migrated significantly slower than those exposed to only CAP or TMZ therapy. The data also showed that TZM treatment appears to cause no significant suppression of α6 and αv integrins when compared to untreated conditions. Whereas CAP, even though several days after plasma treatment, appears to inhibit expression of these integrins in the presence of TMZ. These results suggest that the effect of plasma even though delayed, is permanent. According to previous TMZ studies, inhibition of αv and α6-integrin expression in glioblastoma affects the cell cycle checkpoints and the repair processes in DNA damage. While treatment with TMZ can induce a G_2/M cell cycle arrest [153,154,160,161]. In our study, the data suggested that TMZ treatment induced a delay in the progression of the U87MG. The delay is caused by increasing the number of cells at the G2/M checkpoint 6 days after treatment and in a dose dependent (10-50 μM). Unlike TMZ, CAP does not create a delay in the progression of the cells at the G2/M checkpoint. However, when combined with a drug, it reveals that a larger number of cells are undergoing G2/M cell cycle arrest. These results continue to underline the successful application of plasma in cancer therapy and the ability that it has to counteract glioblastoma cell resistance to TMZ.

5.5 Conclusion

In conclusion, the cytotoxicity of TMZ was amplified with the presence of CAP. For the very first time, we report that TMZ in the presence of CAP induces an inhibition in cell migration, suppressed αv and α6 integrin expression, and G2/M arrest. In summary, the findings reveal compelling evidence in support of the important role played by CAP in mediating cancer suppression through direct treatment or by functioning similarly to drug sensitizing agents.

Chapter 6

Conclusions

1. The biological tissue conductivity, resistance and the amount of applied power play a significant role in the type of burn created by APC treatment. If the resistance of the target tissue were to be outside the range of $0.8 – 3.7\ k\Omega$, an inconsistent amount of power would be delivered, resulting in ineffective treatment or extensive thermal damage. This study suggests that surgeons can adjust the power setting based on the expected resistance of the tissue being treated.
2. It was shown that the adaptive properties of CAP, treatment duration and discharge voltage, play a significant role in mediating cancer suppression *in vitro.* Optimization of CAP operational parameters will be essential in providing long-lasting outcomes in anti-cancer therapy. The adjustment of these paraments caused a reduction in cell viability, which ultimately led to apoptosis potentially via changes in the mitochondrial membrane potential and the rate of protein synthesis**.**
3. Data shows that CAP can improve TMZ treatment outcomes by more significantly increasing cell death in comparison to plasma and TMZ as standalone therapies. The study also presented for the first time the role of CAP in cell migration and integrin expression in the presence of TMZ. CAP induced cell death, G2/M arrest, decreased the rate of cell migration and expression of α6 and αv integrins. The findings revealed compelling evidence in support of the important role played by CAP when functioning similarly to drug sensitizing agents.

6.1 Contributions

The results of this study are published in the following peer-reviewed journals:

a. Gjika, E., Pal-Ghosh, S., Tang, A., Kirschner, M., Tadvalkar, G., Canady, J., Stepp, MA., & Keidar, M. (2018). Adaptation of operational parameters of cold atmospheric plasma for in vitro treatment of cancer cells. *ACS applied materials & interfaces*, *10*(11), 9269-9279.

b. Gjika, E., Scott, D., Shashurin, A., Zhuang, T., Canady, J., & Keidar, M. (2016). Plasma-tissue interactions in argon plasma coagulation: Effects of power and tissue resistance. *Plasma Medicine*, *6*(2).

Relevant work to the topics described in this dissertation published in peer reviewed journals include:

a. Gjika, E., Pekker, M., Shashurin, A., Shneider, M., Zhuang, T., Canady, J., & Keidar, M. (2016). The cutting mechanism of the electrosurgical scalpel. *Journal of Physics D: Applied Physics*, *50*(2), 025401.

b. Lyu, Y., Lin, L., Gjika, E., Lee, T., & Keidar, M. (2019). Mathematical modeling and control for cancer treatment with cold atmospheric plasma jet. *Journal of Physics D: Applied Physics*, *52*(18), 185202.

Manuscript in preparation:

a. The Role of Cold Atmospheric Plasma in Sensitizing Cancer Cells to Temozolomide treatment.

6.2 Future Work

1. Treatment duration and discharge voltage play an important role in adjusting CAP composition and inducing cell death. It has been shown that cell response to CAP treatment varies among different cell lines, and therefore the development of an adaptive CAP platform becomes essential. The concept for this platform was introduced in Chapter 4. The novel platform would rely on the adaptive properties of plasma to develop a feedback mechanism which could lead to improved treatment outcomes.

   Tasks that need to be completed as part of this project include:

   a. Assemble the feedback mechanism platform
   b. Test adaptive platform *in vitro* with real-time monitoring of cell response
   c. Investigate feasibility of utilizing the platform *in vivo* in a mouse model

2. Another interesting ongoing project involves the application of CAP in combination with TMZ in the treatment of glioblastoma in vitro. As part of this project it was shown that CAP can successfully enhance the effect of cytotoxic TMZ doses and sensitize cells to non-cytotoxic TMZ doses. According to the data, CAP in combination with TMZ can affect the expression levels of total α6 and αv integrins. According to the literature, α6β1, αvβ3 and αvβ5 are expressed in U87MG cells therefore to complete this study, expression levels of α6, β3 and β5

will be investigated with flow cytometry. Additional studies will include investigation of different cell lines reported as resistant to TMZ treatment and the investigation of the effect of CAP in the presence of TMZ *in vivo*.

Bibliography

[1] Siegel RL, Miller KD, Jemal A. Cancer statistics, 2016. CA Cancer J Clin 2016;66:7–30. doi:10.3322/caac.21332.

[2] Kayl AE, Meyers CA. Side-effects of chemotherapy and quality of life in ovarian and breast cancer patients. Curr Opin Obstet Gynecol 2006;18:24–8. doi:10.1097/01.gco.0000192996.20040.24.

[3] Siddiqui M, Rajkumar SV. The High Cost of Cancer Drugs and What We Can Do About It. Mayo Clin Proc 2012;87:935. doi:10.1016/J.MAYOCP.2012.07.007.

[4] Money S, Garber B. Management of Cancer Pain. Curr Emerg Hosp Med Rep 2018;6:141–6. doi:10.1007/s40138-018-0170-9.

[5] Zugazagoitia J, Guedes C, Ponce S, Ferrer I, Molina-Pinelo S, Paz-Ares L. Current Challenges in Cancer Treatment. Clin Ther 2016;38:1551–66. doi:10.1016/J.CLINTHERA.2016.03.026.

[6] Tanaka H, Mizuno M, Ishikawa K, Toyokuni S, Kajiyama H, Kikkawa F, et al. New Hopes for Plasma-Based Cancer Treatment. Plasma 2018;1:150–5. doi:10.3390/plasma1010014.

[7] Heinlin J, Isbary G, Stolz W, Morfill G, Landthaler M, Shimizu T, et al. Plasma applications in medicine with a special focus on dermatology 2011:1–11. doi:10.1111/j.1468-3083.2010.03702.x.

[8] Pinheiro MJ. Plasma: the genesis of the word 2007:6–7.

[9] Chukhlantsev KI. Development of plasma-generating devices and history of plasma utilization 2018:1–6.

[10] Machala Z, Pavlovich MJ. A New Phase in Applied Biology. Trends Biotechnol 2018;36:577–8. doi:10.1016/J.TIBTECH.2018.04.001.

[11] Hoffmann C, Berganza C, Zhang J. Cold Atmospheric Plasma: methods of production and application in dentistry and oncology. Med Gas Res 2013;3:21. doi:10.1186/2045-9912-3-21.

[12] Ginsberg GG, Barkun AN, Bosco JJ, Burdick JS, Isenberg GA, Nakao NL, et al. The argon plasma coagulatorFebruary 2002. Gastrointest Endosc 2002;55:807–10. doi:10.1016/S0016-5107(02)70408-2.

[13] von Woedtke T, Reuter S, Masur K, Weltmann K-D. Plasmas for medicine. Phys Rep 2013;530:291–320. doi:10.1016/j.physrep.2013.05.005.

[14] Fridman G, Peddinghaus M, Balasubramanian M, Ayan H, Fridman A, Gutsol A, et al. Blood Coagulation and Living Tissue Sterilization by Floating-Electrode Dielectric Barrier Discharge in Air. Plasma Chem Plasma Process 2006;26:425–42. doi:10.1007/s11090-006-9024-4.

[15] Keidar M, Shashurin A, Volotskova O, Stepp MA, Srinivasan P, Homepage J, et al. Cold atmospheric plasma in cancer therapy Additional information on Phys. Plasmas Cold atmospheric plasma in cancer therapy a). Cit Phys Plasmas 2013;20:57101. doi:10.1063/1.4801516.

[16] Brandenburg R. Dielectric barrier discharges: progress on plasma sources and on the understanding of regimes and single filaments. Plasma Sources Sci Technol 2017;26:053001. doi:10.1088/1361-6595/aa6426.

[17] Kogelschatz U. Dielectric-Barrier Discharges: Their History, Discharge Physics, and Industrial Applications. Plasma Chem Plasma Process 2003;23:1–46.

doi:10.1023/A:1022470901385.

[18] Fridman A, Chirokov A, Gutsol A. Non-thermal atmospheric pressure discharges. J Phys D Appl Phys 2005;38:R1–24. doi:10.1088/0022-3727/38/2/R01.

[19] Raiser J, Zenker M. Argon plasma coagulation for open surgical and endoscopic applications: state of the art. J Phys D Appl Phys 2006;39:3520–3. doi:10.1088/0022-3727/39/16/S10.

[20] Vargo JJ. Clinical applications of the argon plasma coagulator. Gastrointest Endosc 2004;59:81–8. doi:10.1016/S0016-5107(03)02296-X.

[21] Ramakrishnan S, S. Technological Challenges in Thermal Plasma Production. Aust J Phys 1995;48:377. doi:10.1071/PH950377.

[22] Weltmann KD, Kindel E, Woedtke T Von, Hähnel M, Stieber M, Brandenburg R. Atmospheric-pressure plasma sources : Prospective tools for plasma medicine * 2010;82:1223–37. doi:10.1351/PAC-CON-09-10-35.

[23] Lu X, Naidis GV, Laroussi M, Reuter S, Graves DB, Ostrikov K. Reactive species in non-equilibrium atmospheric-pressure plasmas: Generation, transport, and biological effects. Phys Rep 2016;630:1–84. doi:10.1016/J.PHYSREP.2016.03.003.

[24] Reuter S, von Woedtke T, Weltmann K-D. The kINPen—a review on physics and chemistry of the atmospheric pressure plasma jet and its applications. J Phys D Appl Phys 2018;51:233001. doi:10.1088/1361-6463/aab3ad.

[25] Weltmann K-D, Polak M, Masur K, von Woedtke T, Winter J, Reuter S. Plasma Processes and Plasma Sources in Medicine. Contrib to Plasma Phys 2012;52:644–54. doi:10.1002/ctpp.201210061.

[26] Grund KE, Storek D, Farin G. Endoscopic argon plasma coagulation (APC) first clinical experiences in flexible endoscopy. Endosc Surg Allied Technol 1994;2:42–6.

[27] Norton ID, Wang L, Levine SA, Burgart LJ, Hofmeister EK, Yacavone RF, et al. In vivo characterization of colonic thermal injury caused by argon plasma coagulation. Gastrointest Endosc 2002;55:631–6. doi:10.1067/MGE.2002.123418.

[28] Keidar M, Beilis I. Plasma Engineering : Applications from Aerospace to Bio and Nanotechnology. Elsevier Science; 2013.

[29] Brand CU, Blum a, Schlegel a, Farin G, Garbe C. Application of argon plasma coagulation in skin surgery. Dermatology 1998;197:152–7. doi:10.1159/000017988.

[30] Massarweh NN, Cosgriff N, Slakey DP. Electrosurgery: History, principles, and current and future uses. J Am Coll Surg 2006;202:520–30. doi:10.1016/j.jamcollsurg.2005.11.017.

[31] Bolliger CT, Sutedja TG, Strausz J, Freitag L. Therapeutic bronchoscopy with immediate effect: laser, electrocautery, argon plasma coagulation and stents. Eur Respir J 2006;27:1258–71. doi:10.1183/09031936.06.00013906.

[32] Kieft IE, Broers JLV, Caubet-Hilloutou V, Slaaf DW, Ramaekers FCS, Stoffels E. Electric discharge plasmas influence attachment of cultured CHO K1 cells. Bioelectromagnetics 2004;25:362–8. doi:10.1002/bem.20005.

[33] Kieft IE, Darios D, Roks AJM, Stoffels E. Plasma treatment of mammalian vascular cells: a quantitative description. IEEE Trans Plasma Sci 2005;33:771–5. doi:10.1109/TPS.2005.844528.

[34] Schlegel J, Köritzer J, Boxhammer V. Plasma in cancer treatment. Clin Plasma Med 2013;1:2–7. doi:10.1016/J.CPME.2013.08.001.

[35] Shashurin A, Keidar M, Bronnikov S, Jurjus RA, Stepp MA. Living tissue under treatment of cold plasma atmospheric jet. Appl Phys Lett 2008;93:181501. doi:10.1063/1.3020223.

[36] Fridman G, Shereshevsky A, Jost MM, Brooks AD, Fridman A, Gutsol A, et al. Floating Electrode Dielectric Barrier Discharge Plasma in Air Promoting Apoptotic Behavior in Melanoma Skin Cancer Cell Lines. Plasma Chem Plasma Process 2007;27:163–76. doi:10.1007/s11090-007-9048-4.

[37] Zhang X, Li M, Zhou R, Feng K, Yang S. Ablation of liver cancer cells in vitro by a plasma needle. Appl Phys Lett 2008;93:021502. doi:10.1063/1.2959735.

[38] Barekzi N, Laroussi M. Dose-dependent killing of leukemia cells by low-temperature plasma. J Phys D Appl Phys 2012;45:422002. doi:10.1088/0022-3727/45/42/422002.

[39] Walk RM, Snyder JA, Srinivasan P, Kirsch J, Diaz SO, Blanco FC, et al. Cold atmospheric plasma for the ablative treatment of neuroblastoma. J Pediatr Surg 2013;48:67–73. doi:10.1016/J.JPEDSURG.2012.10.020.

[40] Arndt S, Wacker E, Li Y-F, Shimizu T, Thomas HM, Morfill GE, et al. Cold atmospheric plasma, a new strategy to induce senescence in melanoma cells. Exp Dermatol 2013;22:284–9. doi:10.1111/exd.12127.

[41] Kim C-H, Bahn JH, Lee S-H, Kim G-Y, Jun S-I, Lee K, et al. Induction of cell growth arrest by atmospheric non-thermal plasma in colorectal cancer cells. J Biotechnol 2010;150:530–8. doi:10.1016/J.JBIOTEC.2010.10.003.

[42] Wang M, Holmes B, Cheng X, Zhu W, Keidar M, Zhang LG. Cold Atmospheric Plasma for Selectively Ablating Metastatic Breast Cancer Cells. PLoS One 2013;8:e73741. doi:10.1371/journal.pone.0073741.

[43] Vandamme M, Robert E, Dozias S, Sobilo J, Lerondel S, Le Pape A, et al. Response of Human Glioma U87 Xenografted on Mice to Non Thermal Plasma Treatment. Plasma Med 2011;1:27–43. doi:10.1615/PlasmaMed.v1.i1.30.

[44] Keidar M, Walk R, Shashurin A, Srinivasan P, Sandler A, Dasgupta S, et al. Cold plasma selectivity and the possibility of a paradigm shift in cancer therapy. Br J Cancer 2011;105:1295–301. doi:10.1038/bjc.2011.386.

[45] Dai X, Bazaka K, Richard DJ, Thompson E (Rik) W, Ostrikov K (Ken). The Emerging Role of Gas Plasma in Oncotherapy. Trends Biotechnol 2018;36:1183–98. doi:10.1016/J.TIBTECH.2018.06.010.

[46] Keidar M, Shashurin A, Volotskova O, Ann Stepp M, Srinivasan P, Sandler A, et al. Cold atmospheric plasma in cancer therapy. Phys Plasmas 2013;20:057101. doi:10.1063/1.4801516.

[47] System and Method for Electrosurgical Conductive Gas Cutting for Improving Eschar, Sealing Vessels and Tissues 2011.

[48] Scott, D.; Shashurin, A.; Canady, J.; Keidar M. Temporal Evolution of the Discharge in U.S. Medical Innovations Electrosurgical System SS-200E/Argon-2. Plasma Sci IEEE Trans 2014;42:2742,2743.

[49] Volotskova O, Hawley TS, Stepp MA, Keidar M. Targeting the cancer cell cycle by cold atmospheric plasma. Sci Rep 2012;2:636. doi:10.1038/srep00636.

[50] Volotskova O, Shashurin A, Stepp MA, Pal-Ghosh S, Keidar M. Plasma-

Controlled Cell Migration: Localization of Cold Plasma-Cell Interaction Region. Plasma Med 2011;1:85–92. doi:10.1615/PlasmaMed.v1.i1.70.

[51] Lin L, Lyu Y, Shneider MN, Keidar M. Average electron temperature estimation of streamer discharge in ambient air. Rev Sci Instrum 2018;89:113502. doi:10.1063/1.5027836.

[52] Lin L, Lyu Y, Trink B, Canady J, Keidar M. Cold atmospheric helium plasma jet in humid air environment. J Appl Phys 2019;125:153301. doi:10.1063/1.5086177.

[53] Canady J, Wiley K, Ravo B. Argon plasma coagulation and the future applications for dual-mode endoscopic probes. Rev Gastroenterol Disord 2006;6:1.

[54] Laursen S, Schaffalitzky de Muckadell O. Endoscopic Management of Nonvariceal Upper Gastrointestinal Bleeding. Video J Encycl GI Endosc 2013;1:122–4. doi:10.1016/S2212-0971(13)70053-0.

[55] Malick KJ. Clinical applications of argon plasma coagulation in endoscopy. Gastroenterol Nurs 2006;29:386-91; quiz 392-3. doi:10.1097/00001610-200609000-00006.

[56] Kaassis M, Oberti F, Burtin P, Boyer J. Argon Plasma Coagulation for the Treatment of Hemorrhagic Radiation Proctitis. Endoscopy 2000;32:673–6. doi:10.1055/s-2000-9023.

[57] Grade AJ, Shah IA, Medlin SM, Ramirez FC. The efficacy and safety of argon plasma coagulation therapy in Barrett's esophagus. Gastrointest Endosc 1999;50:18–22. doi:10.1016/S0016-5107(99)70338-X.

[58] Sagawa T, Takayama T, Oku T, Hayashi T, Ota H, Okamoto T, et al. Argon plasma coagulation for successful treatment of early gastric cancer with

intramucosal invasion. Gut 2003;52:334–9. doi:10.1136/gut.52.3.334.

[59] Byrne JP, Armstrong GR, Attwood SE a. Restoration of the normal squamous lining in barrett's esophagus by argon beam plasma coagulation. Am J Gastroenterol 1998;93:1810–5. doi:10.1111/j.1572-0241.1998.525_b.x.

[60] Yusoff I, Brennan F, Ormonde D, Laurence B. Argon plasma coagulation for treatment of watermelon stomach. Endoscopy 2002;34:407–10. doi:10.1055/s-2002-25287.

[61] Shashurin A, Scott D, Zhuang T, Canady J, Beilis II, Keidar M. Electric discharge during electrosurgery. Sci Rep 2015;5:9946. doi:10.1038/srep09946.

[62] Canady J, Shashurin A, Wiley K, Fisch NJ, Keidar M. Characterization of Plasma Parameters and Tissue Injury Produced by Plasma Electrosurgical Systems 2013;3:279–89.

[63] Goulet CJ, Disario JA, Emerson L, Hilden K, Holubkov R, Fang JC. In vivo evaluation of argon plasma coagulation in a porcine model 2007;65:457–62. doi:10.1016/j.gie.2006.09.005.

[64] Saul C, Toneloto EB, Rynkowski CB, Blaya C, Alegre P. High power setting argon plasma coagulation for the eradication of Barrett ' s esophagus. Am J Gastroenterol 2000;95:1661–8.

[65] Wahab PJ, Mulder CJJ, den Hartog G, Thies JE. Argon Plasma Coagulation in Flexible Gastrointestinal Endoscopy: Pilot Experiences. Endoscopy 1997;29:176–81. doi:10.1055/s-2007-1004159.

[66] Bodakian B, Hart FX. Dielectric properties of meat. IEEE Trans Dielectr Electr Insul 1994;1:181–7. doi:10.1109/94.300250.

[67] Haemmerich D, Schutt DJ, Wright AW, Webster JG, Mahvi DM. Electrical conductivity measurement of excised human metastatic liver tumours before and after thermal ablation. Physiol Meas 2009;30:459–66. doi:10.1088/0967-3334/30/5/003.

[68] Miklavcic D, Pavselj N, Hart F. Electric properties of tissues. 2006.

[69] Burger HC, Dongen R van. Specific Electric Resistance of Body Tissues. Phys Med Biol 1961;5:304. doi:10.1088/0031-9155/5/4/304.

[70] Schwan HP, Kay CF. THE CONDUCTIVITY OF LIVING TISSUES. Ann N Y Acad Sci 1957;65:1007–13. doi:10.1111/j.1749-6632.1957.tb36701.x.

[71] Gabriel S, Lau RW, Gabriel C. The dielectric properties of biological tissues: II. Measurements in the frequency range 10 Hz to 20 GHz. Phys Med Biol 1996;41:2251–69. doi:10.1088/0031-9155/41/11/002.

[72] Gabriel C, Peyman a, Grant EH. Electrical conductivity of tissue at frequencies below 1 MHz. Phys Med Biol 2009;54:4863–78. doi:10.1088/0031-9155/54/16/002.

[73] Gabriel C, Gabriel S, Corthout E. The dielectric properties of biological tissues: I. Literature survey. Phys Med Biol 1996;41:2231–49. doi:10.1088/0031-9155/41/11/001.

[74] Search H, Journals C, Contact A, Iopscience M, Address IP. Contact us My IOPscience The electric resistivity of human tissues (100 Hz-10 MHz): a meta-analysis of review studies The electric resistivity of human tissues (100 Hz – 10 MHz): a meta-analysis of review studies 1999;1:0–10.

[75] Faes TJC, Meij HA van der, Munck JC de, Heethaar RM. The electric resistivity of

human tissues (100 Hz-10 MHz): a meta-analysis of review studies. Physiol Meas 1999;20:R1–10. doi:10.1088/0967-3334/20/4/201.

[76] Shashurin A, Scott D, Zhuang T, Canady J, Beilis II, Keidar M. Electric discharge during electrosurgery. Sci Rep 2015;4:9946. doi:10.1038/srep09946.

[77] Keidar M, Yan D, Beilis II, Trink B, Sherman JH. Plasmas for Treating Cancer: Opportunities for Adaptive and Self-Adaptive Approaches. Trends Biotechnol 2018;36:586–93. doi:10.1016/J.TIBTECH.2017.06.013.

[78] Stoffels E, Kieft IE, Sladek REJ, Bedem LJM van den, Laan EP van der, Steinbuch M. Plasma needle for in vivo medical treatment: recent developments and perspectives. Plasma Sources Sci Technol 2006;15:S169–80. doi:10.1088/0963-0252/15/4/S03.

[79] Chen Z, Simonyan H, Cheng X, Gjika E, Lin L, Canady J, et al. A Novel Micro Cold Atmospheric Plasma Device for Glioblastoma Both In Vitro and In Vivo. Cancers (Basel) 2017;9:61. doi:10.3390/cancers9060061.

[80] Keidar M. Plasma for cancer treatment. Plasma Sources Sci Technol 2015;24:033001. doi:10.1088/0963-0252/24/3/033001.

[81] Wagenaars E, Gans T, O'Connell D, Niemi K. Two-photon absorption laser-induced fluorescence measurements of atomic nitrogen in a radio-frequency atmospheric-pressure plasma jet. Plasma Sources Sci Technol 2012;21:042002. doi:10.1088/0963-0252/21/4/042002.

[82] Waskoenig J, Niemi K, Knake N, Graham LM, Reuter S, Gathen VS der, et al. Atomic oxygen formation in a radio-frequency driven micro-atmospheric pressure plasma jet. Plasma Sources Sci Technol 2010;19:045018. doi:10.1088/0963-

0252/19/4/045018.

[83] Knake N, Niemi K, Reuter S, Schulz-von der Gathen V, Winter J. Absolute atomic oxygen density profiles in the discharge core of a microscale atmospheric pressure plasma jet. Appl Phys Lett 2008;93:131503. doi:10.1063/1.2995983.

[84] Ninomiya K, Ishijima T, Imamura M, Yamahara T, Enomoto H, Takahashi K, et al. Evaluation of extra- and intracellular OH radical generation, cancer cell injury, and apoptosis induced by a non-thermal atmospheric-pressure plasma jet. J Phys D Appl Phys 2013;46:425401. doi:10.1088/0022-3727/46/42/425401.

[85] Sousa JS, Niemi K, Cox LJ, Algwari QT, Gans T, O'Connell D. Cold atmospheric pressure plasma jets as sources of singlet delta oxygen for biomedical applications. J Appl Phys 2011;109:123302. doi:10.1063/1.3601347.

[86] Kang SU, Cho J-H, Chang JW, Shin YS, Kim KI, Park JK, et al. Nonthermal plasma induces head and neck cancer cell death: the potential involvement of mitogen-activated protein kinase-dependent mitochondrial reactive oxygen species. Cell Death Dis 2014;5:e1056–e1056. doi:10.1038/cddis.2014.33.

[87] Ma Y, Ha CS, Hwang SW, Lee HJ, Kim GC, Lee K-W, et al. Non-Thermal Atmospheric Pressure Plasma Preferentially Induces Apoptosis in p53-Mutated Cancer Cells by Activating ROS Stress-Response Pathways. PLoS One 2014;9:e91947. doi:10.1371/journal.pone.0091947.

[88] Conway GE, Casey A, Milosavljevic V, Liu Y, Howe O, Cullen PJ, et al. Non-thermal atmospheric plasma induces ROS-independent cell death in U373MG glioma cells and augments the cytotoxicity of temozolomide. Br J Cancer 2016;114:435–43. doi:10.1038/bjc.2016.12.

[89] Hirst AM, Simms MS, Mann VM, Maitland NJ, O'Connell D, Frame FM. Low-temperature plasma treatment induces DNA damage leading to necrotic cell death in primary prostate epithelial cells. Br J Cancer 2015;112:1536–45. doi:10.1038/bjc.2015.113.

[90] Graves DB. The emerging role of reactive oxygen and nitrogen species in redox biology and some implications for plasma applications to medicine and biology. J Phys D Appl Phys 2012;45:263001. doi:10.1088/0022-3727/45/26/263001.

[91] Yan D, Sherman JH, Cheng X, Ratovitski E, Canady J, Keidar M. Controlling plasma stimulated media in cancer treatment application. Appl Phys Lett 2014;105:224101. doi:10.1063/1.4902875.

[92] GUERRERO-PRESTON R, OGAWA T, UEMURA M, SHUMULINSKY G, VALLE BL, PIRINI F, et al. Cold atmospheric plasma treatment selectively targets head and neck squamous cell carcinoma cells. Int J Mol Med 2014;34:941–6. doi:10.3892/ijmm.2014.1849.

[93] Brullé L, Vandamme M, Riès D, Martel E, Robert E, Lerondel S, et al. Effects of a Non Thermal Plasma Treatment Alone or in Combination with Gemcitabine in a MIA PaCa2-luc Orthotopic Pancreatic Carcinoma Model. PLoS One 2012;7:e52653. doi:10.1371/journal.pone.0052653.

[94] Partecke LI, Evert K, Haugk J, Doering F, Normann L, Diedrich S, et al. Tissue Tolerable Plasma (TTP) induces apoptosis in pancreatic cancer cells in vitro and in vivo. BMC Cancer 2012;12:473. doi:10.1186/1471-2407-12-473.

[95] Zucker SN, Zirnheld J, Bagati A, DiSanto TM, Des Soye B, Wawrzyniak JA, et al. Preferential induction of apoptotic cell death in melanoma cells as compared with

normal keratinocytes using a non-thermal plasma torch. Cancer Biol Ther 2012;13:1299–306. doi:10.4161/cbt.21787.

[96] Georgescu N, Lupu AR. Tumoral and Normal Cells Treatment With High-Voltage Pulsed Cold Atmospheric Plasma Jets. IEEE Trans Plasma Sci 2010;38:1949–55. doi:10.1109/TPS.2010.2041075.

[97] Zirnheld JL, Zucker SN, DiSanto TM, Berezney R, Etemadi K. Nonthermal Plasma Needle: Development and Targeting of Melanoma Cells. IEEE Trans Plasma Sci 2010;38:948–52. doi:10.1109/TPS.2010.2041470.

[98] Ahn HJ, Kim K Il, Kim G, Moon E, Yang SS, Lee J-S. Atmospheric-Pressure Plasma Jet Induces Apoptosis Involving Mitochondria via Generation of Free Radicals. PLoS One 2011;6:e28154. doi:10.1371/journal.pone.0028154.

[99] Leduc M, Guay D, Leask RL, Coulombe S. Cell permeabilization using a non-thermal plasma. New J Phys 2009;11:115021. doi:10.1088/1367-2630/11/11/115021.

[100] Kim SJ, Chung TH, Bae SH, Leem SH. Induction of apoptosis in human breast cancer cells by a pulsed atmospheric pressure plasma jet. Appl Phys Lett 2010;97:023702. doi:10.1063/1.3462293.

[101] Wang M, Holmes B, Cheng X, Zhu W, Keidar M, Zhang LG. Cold Atmospheric Plasma for Selectively Ablating Metastatic Breast Cancer Cells. PLoS One 2013;8:e73741. doi:10.1371/journal.pone.0073741.

[102] Murphy KM, Ranganathan V, Farnsworth ML, Kavallaris M, Lock RB. Bcl-2 inhibits Bax translocation from cytosol to mitochondria during drug-induced apoptosis of human tumor cells. Cell Death Differ 2000;7:102–11.

doi:10.1038/sj.cdd.4400597.

[103] Buszczak M, Signer RAJ, Morrison SJ. Cellular Differences in Protein Synthesis Regulate Tissue Homeostasis. Cell 2014;159:242–51. doi:10.1016/J.CELL.2014.09.016.

[104] Ahn HJ, Kim K Il, Hoan NN, Kim CH, Moon E, Choi KS, et al. Targeting Cancer Cells with Reactive Oxygen and Nitrogen Species Generated by Atmospheric-Pressure Air Plasma. PLoS One 2014;9:e86173. doi:10.1371/journal.pone.0086173.

[105] Graves DB. Low temperature plasma biomedicine: A tutorial review. Phys Plasmas 2014;21:080901. doi:10.1063/1.4892534.

[106] Kalghatgi S, Friedman G, Fridman A, Clyne AM. Endothelial Cell Proliferation is Enhanced by Low Dose Non-Thermal Plasma Through Fibroblast Growth Factor-2 Release. Ann Biomed Eng 2010;38:748–57. doi:10.1007/s10439-009-9868-x.

[107] Dreher D, Junod AF. Role of oxygen free radicals in cancer development. Eur J Cancer 1996;32:30–8. doi:10.1016/0959-8049(95)00531-5.

[108] Diehn M, Cho RW, Lobo NA, Kalisky T, Dorie MJ, Kulp AN, et al. Association of reactive oxygen species levels and radioresistance in cancer stem cells. Nature 2009;458:780–3. doi:10.1038/nature07733.

[109] Gorrini C, Harris IS, Mak TW. Modulation of oxidative stress as an anticancer strategy. Nat Rev Drug Discov 2013;12:931–47. doi:10.1038/nrd4002.

[110] Xiong S, Mu T, Wang G, Jiang X. Mitochondria-mediated apoptosis in mammals. Protein Cell 2014;5:737–49. doi:10.1007/s13238-014-0089-1.

[111] Zhao J, Zhang L, Li J, Wu T, Wang M, Xu G, et al. A novel pyrazolone-based

derivative induces apoptosis in human esophageal cells via reactive oxygen species (ROS) generation and caspase-dependent mitochondria-mediated pathway. Chem Biol Interact 2015;231:1–9. doi:10.1016/J.CBI.2015.02.004.

[112] Magni L, Raimondo DM, Allgöwer F, editors. Nonlinear Model Predictive Control. vol. 384. Berlin, Heidelberg: Springer Berlin Heidelberg; 2009. doi:10.1007/978-3-642-01094-1.

[113] Murphy W, Carroll C, Keidar M. Simulation of the effect of plasma species on tumor growth and apoptosis. J Phys D Appl Phys 2014;47:472001. doi:10.1088/0022-3727/47/47/472001.

[114] Friedman HS, Kerby T, Calvert H. Temozolomide and treatment of malignant glioma. Clin Cancer Res 2000;6:2585–97.

[115] Stupp R, Mason WP, van den Bent MJ, Weller M, Fisher B, Taphoorn MJB, et al. Radiotherapy plus Concomitant and Adjuvant Temozolomide for Glioblastoma. N Engl J Med 2005;352:987–96. doi:10.1056/NEJMoa043330.

[116] Hegi ME, Diserens A-C, Gorlia T, Hamou M-F, de Tribolet N, Weller M, et al. *MGMT* Gene Silencing and Benefit from Temozolomide in Glioblastoma. N Engl J Med 2005;352:997–1003. doi:10.1056/NEJMoa043331.

[117] Silber JR, Bobola MS, Blank A, Chamberlain MC. O6-Methylguanine-DNA methyltransferase in glioma therapy: Promise and problems. Biochim Biophys Acta - Rev Cancer 2012;1826:71–82. doi:10.1016/J.BBCAN.2011.12.004.

[118] Martin S, Janouskova H, Dontenwill M. Integrins and p53 pathways in glioblastoma resistance to temozolomide. Front Oncol 2012;2:157. doi:10.3389/fonc.2012.00157.

[119] Brandes AA, Tosoni A, Franceschi E, Reni M, Gatta G, Vecht C. Glioblastoma in adults. Crit Rev Oncol Hematol 2008;67:139–52. doi:10.1016/j.critrevonc.2008.02.005.

[120] Lee SY. Temozolomide resistance in glioblastoma multiforme. Genes Dis 2016;3:198–210. doi:10.1016/j.gendis.2016.04.007.

[121] Kim SJ, Chung TH. Cold atmospheric plasma jet-generated RONS and their selective effects on normal and carcinoma cells. Sci Rep 2016;6:20332. doi:10.1038/srep20332.

[122] Utsumi F, Kajiyama H, Nakamura K, Tanaka H, Hori M, Kikkawa F. Selective cytotoxicity of indirect nonequilibrium atmospheric pressure plasma against ovarian clear-cell carcinoma. Springerplus 2014;3:398. doi:10.1186/2193-1801-3-398.

[123] Vandamme M, Robert E, Lerondel S, Sarron V, Ries D, Dozias S, et al. ROS implication in a new antitumor strategy based on non-thermal plasma. Int J Cancer 2012;130:2185–94. doi:10.1002/ijc.26252.

[124] Lin L, Wang L, Liu Y, Xu C, Tu Y, Zhou J, et al. Non-thermal plasma inhibits tumor growth and proliferation and enhances the sensitivity to radiation invitro and invivo. Oncol Rep 2018;40:3405–15. doi:10.3892/or.2018.6749.

[125] Aoudjit F, Vuori K. Integrin Signaling in Cancer Cell Survival and Chemoresistance. Chemother Res Pract 2012;2012:1–16. doi:10.1155/2012/283181.

[126] Hodkinson PS, Elliott T, Wong WS, Rintoul RC, Mackinnon AC, Haslett C, et al. ECM overrides DNA damage-induced cell cycle arrest and apoptosis in small-cell

lung cancer cells through β1 integrin-dependent activation of PI3-kinase. Cell Death Differ 2006;13:1776–88. doi:10.1038/sj.cdd.4401849.

[127] Park J, Lee H, Lee HJ, Kim GC, Kim DY, Han S, et al. Non-Thermal Atmospheric Pressure Plasma Efficiently Promotes the Proliferation of Adipose Tissue-Derived Stem Cells by Activating NO-Response Pathways. Sci Rep 2016;6:39298. doi:10.1038/srep39298.

[128] Christmann M, Diesler K, Majhen D, Steigerwald C, Berte N, Freund H, et al. Integrin αVβ3 silencing sensitizes malignant glioma cells to temozolomide by suppression of homologous recombination repair. Oncotarget 2017;8:27754–71. doi:10.18632/oncotarget.10897.

[129] Meldolesi J. Pharmacology of the cell/matrix form of adhesion. Pharmacol Res 2016;107:430–6. doi:10.1016/J.PHRS.2015.10.019.

[130] Bianconi D, Unseld M, Prager G, Bianconi D, Unseld M, Prager GW. Integrins in the Spotlight of Cancer. Int J Mol Sci 2016;17:2037. doi:10.3390/ijms17122037.

[131] Hynes RO. Integrins: Bidirectional, Allosteric Signaling Machines. Cell 2002;110:673–87. doi:10.1016/S0092-8674(02)00971-6.

[132] Thomas GJ, Lewis MP, Whawell SA, Russell A, Sheppard D, Hart IR, et al. Expression of the αvβ6 Integrin Promotes Migration and Invasion in Squamous Carcinoma Cells. J Invest Dermatol 2001;117:67–73. doi:10.1046/J.0022-202X.2001.01379.X.

[133] Paolillo M, Serra M, Schinelli S. Integrins in glioblastoma: Still an attractive target? Pharmacol Res 2016;113:55–61. doi:10.1016/j.phrs.2016.08.004.

[134] Li Y, Ho Kang M, Sup Uhm H, Joon Lee G, Ha Choi E, Han I. Effects of

atmospheric-pressure non-thermal bio-compatible plasma and plasma activated nitric oxide water on cervical cancer cells. Sci Rep 2017;7:45781. doi:10.1038/srep45781.

[135] Liedtke KR, Bekeschus S, Kaeding A, Hackbarth C, Kuehn J-P, Heidecke C-D, et al. Non-thermal plasma-treated solution demonstrates antitumor activity against pancreatic cancer cells in vitro and in vivo. Sci Rep 2017;7:8319. doi:10.1038/s41598-017-08560-3.

[136] Nakamura K, Peng Y, Utsumi F, Tanaka H, Mizuno M, Toyokuni S, et al. Novel Intraperitoneal Treatment With Non-Thermal Plasma-Activated Medium Inhibits Metastatic Potential of Ovarian Cancer Cells. Sci Rep 2017;7:6085. doi:10.1038/s41598-017-05620-6.

[137] Liu Y, Tan S, Zhang H, Kong X, Ding L, Shen J, et al. Selective effects of non-thermal atmospheric plasma on triple-negative breast normal and carcinoma cells through different cell signaling pathways. Sci Rep 2017;7:7980. doi:10.1038/s41598-017-08792-3.

[138] Yu H, Wang Y, Wang S, Li X, Li W, Ding D, et al. Paclitaxel-Loaded Core–Shell Magnetic Nanoparticles and Cold Atmospheric Plasma Inhibit Non-Small Cell Lung Cancer Growth. ACS Appl Mater Interfaces 2018;10:43462–71. doi:10.1021/acsami.8b16487.

[139] Cheng X, Sherman J, Murphy W, Ratovitski E, Canady J, Keidar M. The Effect of Tuning Cold Plasma Composition on Glioblastoma Cell Viability. PLoS One 2014;9:e98652. doi:10.1371/journal.pone.0098652.

[140] Siu A, Volotskova O, Cheng X, Khalsa SS, Bian K, Murad F, et al. Differential

Effects of Cold Atmospheric Plasma in the Treatment of Malignant Glioma. PLoS One 2015;10:e0126313. doi:10.1371/journal.pone.0126313.

[141] Massagué J. G1 cell-cycle control and cancer. Nature 2004;432:298–306. doi:10.1038/nature03094.

[142] Kastan MB, Bartek J. Cell-cycle checkpoints and cancer. Nature 2004;432:316–23. doi:10.1038/nature03097.

[143] Hegi ME, Diserens A-C, Gorlia T, Hamou M-F, de Tribolet N, Weller M, et al. *MGMT* Gene Silencing and Benefit from Temozolomide in Glioblastoma. N Engl J Med 2005;352:997–1003. doi:10.1056/NEJMoa043331.

[144] Goellner EM, Grimme B, Brown AR, Lin Y-C, Wang X-H, Sugrue KF, et al. Overcoming temozolomide resistance in glioblastoma via dual inhibition of NAD+ biosynthesis and base excision repair. Cancer Res 2011;71:2308–17. doi:10.1158/0008-5472.CAN-10-3213.

[145] Marosi C. Complications of chemotherapy in neuro-oncology. Handb. Clin. Neurol., vol. 105, 2012, p. 873–85. doi:10.1016/B978-0-444-53502-3.00029-X.

[146] Castro GN, Cayado-Gutiérrez N, Zoppino FCM, Fanelli MA, Cuello-Carrión FD, Sottile M, et al. Effects of temozolomide (TMZ) on the expression and interaction of heat shock proteins (HSPs) and DNA repair proteins in human malignant glioma cells. Cell Stress Chaperones 2015;20:253–65. doi:10.1007/s12192-014-0537-0.

[147] Köritzer J, Boxhammer V, Schäfer A, Shimizu T, Klämpfl TG, Li Y-F, et al. Restoration of Sensitivity in Chemo — Resistant Glioma Cells by Cold Atmospheric Plasma. PLoS One 2013;8:e64498.

doi:10.1371/journal.pone.0064498.

[148] Patel M, McCully C, Godwin K, Balis FM. Plasma and Cerebrospinal Fluid Pharmacokinetics of Intravenous Temozolomide in Non-human Primates. J Neurooncol 2003;61:203–7. doi:10.1023/A:1022592913323.

[149] Ostermann S, Csajka C, Buclin T, Leyvraz S, Lejeune F, Decosterd LA, et al. Plasma and Cerebrospinal Fluid Population Pharmacokinetics of Temozolomide in Malignant Glioma Patients. Clin Cancer Res 2004;10:3728–36. doi:10.1158/1078-0432.CCR-03-0807.

[150] Zhang D, Tian A, Xue X, Wang M, Qiu B, Wu A, et al. The Effect of Temozolomide/Poly(lactide-co-glycolide) (PLGA)/Nano-Hydroxyapatite Microspheres on Glioma U87 Cells Behavior. Int J Mol Sci 2012;13:1109–25. doi:10.3390/ijms13011109.

[151] Hood JD, Cheresh DA. Role of integrins in cell invasion and migration. Nat Rev Cancer 2002;2:91–100. doi:10.1038/nrc727.

[152] Bello L, Lucini V, Giussani C, Carrabba G, Pluderi M, Scaglione F, et al. IS20I, a Specific αvβ3 Integrin Inhibitor, Reduces Glioma Growth in Vivo. Neurosurgery 2003;52:177–86. doi:10.1227/0006123-200301000-00023.

[153] Malric L, Monferran S, Gilhodes J, Boyrie S, Dahan P, Skuli N, et al. Interest of integrins targeting in glioblastoma according to tumor heterogeneity and cancer stem cell paradigm: an update. Oncotarget 2017;8:86947–68. doi:10.18632/oncotarget.20372.

[154] Kowalski-Chauvel A, Modesto A, Gouaze-andersson V, Baricault L, Gilhodes J, Delmas C, et al. Alpha-6 integrin promotes radioresistance of glioblastoma by

modulating DNA damage response and the transcription factor Zeb1. Cell Death Dis 2018;9:872. doi:10.1038/s41419-018-0853-x.

[155] Blackert S, Haertel B, Wende K, von Woedtke T, Lindequist U. Influence of non-thermal atmospheric pressure plasma on cellular structures and processes in human keratinocytes (HaCaT). J Dermatol Sci 2013;70:173–81. doi:10.1016/J.JDERMSCI.2013.01.012.

[156] Haertel B, Hähnel M, Blackert S, Wende K, von Woedtke T, Lindequist U. Surface molecules on HaCaT keratinocytes after interaction with non-thermal atmospheric pressure plasma. Cell Biol Int 2012;36:1217–22. doi:10.1042/CBI20120139.

[157] Shashurin A, Stepp MA, Hawley TS, Pal-Ghosh S, Brieda L, Bronnikov S, et al. Influence of Cold Plasma Atmospheric Jet on Surface Integrin Expression of Living Cells. Plasma Process Polym 2010;7:294–300. doi:10.1002/ppap.200900086.

[158] Naciri M, Dowling D, Al-Rubeai M. Differential Sensitivity of Mammalian Cell Lines to Non-Thermal Atmospheric Plasma. Plasma Process Polym 2014;11:391–400. doi:10.1002/ppap.201300118.

[159] Volotskova O, Stepp MA, Keidar M. Integrin activation by a cold atmospheric plasma jet. New J Phys 2012;14:053019. doi:10.1088/1367-2630/14/5/053019.

[160] Carduner L, Picot CR, Leroy-Dudal J, Blay L, Kellouche S, Carreiras F. Cell cycle arrest or survival signaling through αv integrins, activation of PKC and ERK1/2 lead to anoikis resistance of ovarian cancer spheroids. Exp Cell Res 2014;320:329–42. doi:10.1016/j.yexcr.2013.11.011.

[161] Chen YK, Jakribettuu V, Springer EW, Shah RJ, Penberthy J, Nash SR. Safety and efficacy of argon plasma coagulation trimming of malpositioned and migrated biliary metal stents: a controlled study in the porcine model. Am J Gastroenterol 2006;101:2025–30. doi:AJG744 [pii]\r10.1111/j.1572-0241.2006.00744.x.